A MODEL ANALYSIS OF SAND INSERTION IN HYDRAULIC FRACTURES

by

YA HAO

Presented to the Faculty of the Graduate School of

The University of Texas at Arlington in Partial Fulfillment

of the Requirements

For the Degree of

MASTER OF SCIENCE IN MECHANICAL ENGINEERING

THE UNIVERSITY OF TEXAS AT ARLINGTON

December 2015

Acknowledgements

I would like to thank Dr. Bo Yang for his supervision, guidance and encouragement in helping me to complete my thesis.

Next, I would like to thank Dr. Chan and Dr. Wang for being members of my committee.

I would like to thank the Department of Mechanical & Aerospace Engineering for giving me the opportunity to pursue my graduate degree in mechanical engineering.

I dedicate this work to my grandmother, Huai Xiang Zhang, my parents, Si Wei Hao and Cai Ping Li, my brother, Dou Hao for their support and encouragement throughout my graduate time.

November 23, 2015

Abstract

A MODEL ANALYSIS OF SAND INSERTION IN HYDRAULIC FRACTURES

YA HAO, MS

The University of Texas at Arlington, 2015

Supervising Professor: Bo Yang

Hydraulic fracturing (fracking) is a well-stimulation technology to create large volume of fracture formation in rocks for gas and/or oil extraction. This technology has been applied to commercially exploit natural gas in unconventional shale reservoirs that contain immense quantity but low density of hydrocarbon sources. The productivity can be largely dependent on the connectivity of fractures that must stay open. However, upon initial hydraulic fracturing, the fractures would be closed due to high hydrostatic pressure deep inside the crust. Sand must be pumped into the fractures to keep them open. An in-depth understanding of the sand distribution and its dependence on operation parameters is essential to keep improving the flow conductivity and hence improving the fracking productivity. In the present study, a model is developed to analyze the sand motion along with hydraulic flow inside an opening crack. The crack opening profile is determined by the hydraulic pressure field meanwhile the hydraulic pressure field is in turn determined by the crack opening profile. They are described by the elastic fracture mechanics theory and the viscous gap flow theory, respectively, and are solved together. Upon the flow field, the sand transport problem is modeled with both inertia and convective effects taken into account. The thermal diffusion is also

considered but determined to be trivial in comparison to those two effects. Parametric studies are carried out in terms of applied hydraulic pressure, fluid viscosity, and sand particle size. It is found that smaller sand particle size, lower fluid viscosity and higher hydraulic pressure can lead to greater depth of sand moving into a fracture. The sand insertion depth and quantity are sensitive to fluid viscosity only when the viscosity is low. The applied hydraulic pressure plays the most important role in moving sand into a fracture, probably because it determines the fracture opening gap. When the fracture is opened more with a higher hydraulic pressure, more sand can be moved in.

Table of Contents

List of Illustrations

List of Tables

Chapter 1

Introduction

1.1 Hydraulic fracturing in shale reservoirs

Hydraulic fracturing is a well-stimulation technology that has been applied to commercially exploit natural gas in the shale reservoir. Because it contains immense quantity and low density hydrocarbon resources, the characters of shale rock demand high conductivity created by hydraulic fracturing, which uses high pressure fluid to pump water, chemicals and proppant into the reservoir. The proppant is typically sand with a demanding size and concentration. After the high engineered fluid cracks the shale rock and flows back to the ground, the proppant is distributed randomly in the fractures to support them openly for conductivity. Since high conductivity of shale rock could contribute high well production, the distribution of proppant is pivotal for well productivity, and determining the most effective proppant characteristics is a practical method to improve the conductivity. Besides the contribution of proppant, the rate, and pressure of the engineered fluid, the components of the fluid are still significant factors needed to be considered.

In the 1860s, dynamite or nitroglycerin detonations were used as a fracturing method to stimulate petroleum reservoir so as to increase oil and gas production. Instead of the explosive detonators in the 1930s, acid was introduced to decrease the fracture's closing speed due to acid etching. In 1947, the first on-site hydraulic fracturing experiment was operated in Kansas with unsuccessful

results. After that, J. B. Clark of Stanolind's further researched the process resulting in a patent and exclusive license for Halliburton. Two years later, the first two wells, in Oklahoma and Texas, were applied commercially by this hydraulic fracturing technology. Massive hydraulic fracturing was first applied in 1968 and successfully extracted gas in the low-permeability sandstone. The definition of massive fracturing is the injection volume of proppant of more than 150 short tons (Ben E. Law and Charles W. Spencer, 1993). Meanwhile, guar-based cross-linked fracturing fluid was successfully employed in the low-permeability well because of its friction reducing and rheological properties. In the late of 1980s, horizontal drilling began to be applied in the oil well at Austin Chalk. Afterwards, slickwater was introduced to increase the fracture of the shale rock. These two methods, horizontal drilling and slickwater, largely improved the overall methods of the fracture up to today.

In the history of fracking, two kinds of fluids, high-viscosity and high rate fluids are applied to transport proppant into the fracture. Water-soluble gelling agents are added to increase viscosity, creating high viscosity fluid, which could keep proppants in suspension, efficiently transport them into the formation, and effectively create larger primary fractures (Andrews, Anthony et al. 2009). However, this method is insufficient to crack complicated and micro-tiny fractures. By contrast, high-rate fracturing fluid, mainly slickwater, can make those complex and minute fractures. "The benefits of slickwater treatments include significantly

reduced gel damage, lower costs, higher fracture-network complexity (shale-gas reservoirs), potential for improved height containment, and environmental advantages (the ability to recycle/reuse both load and produced water) (Palishch, Vincent, and Handren, 2010).” Nevertheless, inefficient proppant transportation and placement are inevitable for slickwater because of its low carrying capacity, even with more high rate and pressure. Hence, proppants are more centralized around the existing dune, which decreases the conductivity of the gas. However, the comprehensive effect of shear displacement, closure stress, in-situ stress, roughness, stress shadow, porous pressure, natural fracture, proppant size and strength, fluid rate and pressure could influence the conductivity at different levels.

1.2 Literature review

Shale fracture conductivity is a critical goal for hydraulic fracturing since well productivity is directly influenced by fracture conductivity. The conductivity is comprehensively effected by the interaction of rock, fracturing fluid and proppant. The physical properties of rock, such as shear displacement, closure stress, in-situ stress, fracture roughness, stress shadow, and porous pressure, could affect the spreading of fractures. Besides that, the distribution of a rock’s natural fracture is a significant factor for fracture propagation. Meanwhile, a fluid’s pumping rate, pressure and chemical composition are necessary to be considered when creating the fracture.

Lastly, proppant size and strength are the critical factors for keeping the fracture open after the energized fluid flows back to the ground.

The physical properties of rock, breakdown pressure, fracture displacement, fracture roughness, in-situ stress, stress shadow, stress anisotropy and porous pressure have been shown in research literature to have a strong influence on fracture conductivity. Guo, Morgenstern and Scott (1993) studied that breakdown is a complicated process that is rate-dependent, size-dependent, fracture fluid-dependent and sigma3-dependent. This four characteristics for breakdown were analyzed experimentally and theoretically by the fracture mechanics model, and proved that breakdown seems to be correlated with the beginning of unstable fracture propagation. Displacement and stress fields around a hydraulic fracture are modeled as a two-dimensional elastic fracture cracked by irregular overpressure, the areas far from the drill site are inclined to be more steady, but closer to the site tends to be more changeable because of the overpressure variation. These observations could estimate the displacement of hydraulic fracturing and stress fields (Kusumoto and Gumundsson, 2014). Raimbay, Babadagli and Kuru (2014) researched the characteristics of fracture roughness in the presence of proppants by cracking seven different kinds of rock samples, the results demonstrate visually and quantitatively that fracture conductivity is controlled by the fractal roughness of the fracture, but pumping the proppants declines the permeability since the distribution of proppants is influenced

by the surface roughness, and substantially decreases the permeability because of roughness and shear stress. According to the research by Warpinski, Schmidt and Northrop (1982), in-situ stresses is the predominant influence on preventing the growth of a hydraulic fracture, which means that fractures are arrested wherever there is insufficient pressure to crack the rock, meanwhile, the material property differences are not critical factors for holding the fracture spread in the mine-back experiments. Wu, Kresse, Weng et al. (2012) developed an unconventional fracture model (UFM) incorporated with shadow calculation to simulate fracture propagation with natural fractures, the stress shadow could significantly decrease the fracture width, rapidly increase pump pressure, change the fracture path and network patterns, however, large perforation friction and fracture spacing could dissipate the effect of a stress shadow, making fractures become more uniform. Based on Fan, Thompson and Robinson's understanding of gas production mechanism and effectiveness of well simulation in the Haynesville shale, high stress anisotropy produces a narrow or linear fracture propagation, on the contrary, complex fracture geometry could be created by the low stress anisotropy. "Theoretical analysis and experimental results are presented to describe the influence of pore pressure on tensile fracture initiation and propagation direction, fracture is influenced by both pore pressure magnitude on a local scale around the crack tip and by the orientation and distribution of pore pressure gradients on a global scale (Bruno and Nakagawa, 1991)."

Besides the physical properties of rock, natural fracture in research literature shows to have an effective influence on fracture conductivity. In the research paper on the Haynesville shale through reservoir simulation by Fan, Thompson, and Robinson (2010), "the open natural fractures provide surface area to help realize the gas from the shale matrix and transport gas into the horizontal wellbore, in other words, natural fractures in the model do not provide enough surface area near the wellbore to match early flush production volume and provide too much surface or drainage area in the reservoir to match the longer term production." The practical conclusion is that in most wellbores, natural fractures are not the primary factor controlling the production. Nevertheless, the preexisting fractures increase complexity of the fracture networks and help the long-term production. Another important area is the crossing of natural and hydraulic fractures. It is better when hydraulic fractures intersect natural fractures when the cross angle is closer to 90 degrees, otherwise, interface slip is more likely to form (Gu, Weng and Lund et al. 2011).

Thirdly, fracture fluid's composition and operation have critical influence on the fracture propagation. According to Kundert, Mullen's summation (2009), keeping the fluid chemistry as simple as possible is a primary principle for the fracture fluid chemical composition. The minimum amount of friction reducer, breaker for the friction reducer, surfactant, biocide, and clay-protection additive are suggested to be used in the hydraulic fracturing. The fracture propagation model

was employed by Wu and Olson (2013) to investigate the impact of the pumping rate for fracking, slickwater treatments at 90 and 120 bpm total rate and gel treatments at 45 and 60 bpm are applied into the experimental comparison. The gel trials have more width and less length than slickwater. The gel trials differed between the exterior and interior fractures because of the higher net pressure and stronger mechanical interactions. By contrast, the net pressure of the slickwater tests was less dependent on bpm rate, and the difference between interior and exterior fracture is less than gel trials.

Lastly, proppant size, strength and concentrations are the critical controllable factors for improving the conductivity and minimizing the uncertainties, such as a rock's formation and physical properties, these uncertainties are difficult to measure yet can have a meaningful impact on the conductivity. Kundert and Mullen (2009) observed that the small mesh-size (40/70) proppant is proposed in the example of slickwater, however, depending on rock permeability, 100-mesh sand might be necessary with naturally fractured shale for improving the conductivity; From a series of laboratory conductivity experiments performed with hydraulically fractured cores from the East Texas Cotton Valley sandstone formation by Fredd, McConnell, Boney et.al (2000), high strength propellants could make the conductivity more proppant dominated and reduce the effects of formation properties even at lower concentrations. The proper selection of proppant should couple the knowledge of proppant transport and fracture complexity,

considering how proppant would perform under the real situation (Palisch, Ceramics, Vincent, et al. 2008).

Currently, laboratory experiments and numerable simulations are the two main methods in analyzing rock properties, fracturing fluid and proppant's effect for conductivity.

1.3 Problem description

The fracture conductivity is the function of fracture permeability and fracture width. Proppant size and strength, fracturing fluid viscosity and composition, pumping rate and pressure are all controllable factors for improving fracture conductivity. However, according to research by Cipolla et al. (2011), 2% to 5% of the total created area is propped which they observed with the unconventional fracture model and wire-mesh model. In this situation, the production only comes from the propped area (Cipolla et al. 2010). Thus, proppant distribution is a critical factor for production in hydraulic fracturing. Hence now it is necessary to analyze the research methods of proppant distribution.

In 1949, the first two hydraulic fracturing treatments occurred at the oil and gas wells in Oklahoma and Texas. However, the research about particle transportation in the hydraulic fracture method is few until the 1950s. One of the first studies about proppant transportation was conducted by Kern et al, in which bed buildup was simulated for the vertical fracture segment in a laboratory. After that, horizontal fractures were studied in the proppant distribution. According to

Lowe. et al (1965), “this laboratory flow study covers propping agent transport in the horizontal fracture as influenced by the characteristics of the propping particles, fluid and fracture.” Around the same time, transport efficiencies of solids in the sand-liquid slurries were investigated in the horizontal fractures. These papers investigated particle movement between two parallel plates with limited vertical fracture conducted by laboratory experiments.

Coming to the 1980s, in theory and lab work, particle setting velocity became a popular research topic for understanding the distribution of propping agent in the hydraulic fracture. At different Reynolds numbers, viscous and elastic properties of the fluid were measured in order to predict proppant settling characteristics, research by Acharya (1984), Clark and Quadir’s (1981). These authors combined theoretical results and experimental data to derive the formulation of settling velocity for a single particle. Meanwhile, the influence from multiple particles was studied to further understand prediction of settling velocity.

Since the 20th Century, proppants group movement are being researched in terms of advection and dispersion, rather than a single particle’s movement. Fractures, fluids and particles are highly integrated into one model to investigate proppant distribution. The most common fracture models are PKN, KGD and Penny-shaped. The fluidity of slickwater is governed by the power law or cubic law, which states particles are forced by inertia, gravity buoyancy, and drag forces (Xiang, 2011). In lab experiments, factors about hydraulic fracture conductivity are

investigated by using real shale and slickwater (Kamenov, 2013). From all of this research, the studies that had computational data coupled with experimental results were more persuasive (Zhang 2014 and Crespo et al. 2013).

However, in all this research, fewer studies focused on the influence of proppant distribution on conductivity, and more research concentrated on the fracture propagation by hydraulic fracturing. This thesis focuses on proppant distribution on conductivity because it demands further study.

This study at hand presents a model analysis of sand insertion in hydraulic fractures. The effects of sand radius, fluid viscosity and pressure are investigated by measuring sand concentration.

1.4 Research objectives

The insertion of proppant in heterogeneous shale formations can be numerically determined by a simulation analysis. This research has the listed objectives:

1. Understand the fluid mechanics in the fracture.
2. Coupling the physical function of proppant and fluid.
3. Study fracture displacement by the function of slickwater.
4. Investigate the factors for proppant insertion.

By accomplishing these objectives, this work assists in understanding sand insertion in the fracture; and a better understanding of the interaction among sand, fluid and rock in the hydraulic fracturing process.

Chapter 2

Technical Review

2.1 Particle modeling tracking

The Eulerian and the Lagrangian model are most commonly used methods in the computational fluid dynamics modeling of particle tracking. Generally, the Eulerian model solves the particles as a concentration continuum phase. In contrast, the Lagrangian model treats the particle as a discrete collection of individual substance.

These two models can be applied into different situations depending on the requirements. If the solution is demanding in terms of a concentration field, the Eulerian model would be more suitable for analyzing the particle as a continuum phase; if the solution is required for each particle's trajectory, the Lagrangian model would be more advantageous than the Eulerian model since an individual particle is tracked, however, statistical analysis is necessary for a relatively precise solution by tracking a large number of particles; when the particle is too big to treat as a continuum phase due to its significant gravity and buoyancy, the Lagrangian model is more useful than the Eulerian model; when advection is more dominant than dispersion, the Lagrangian model is suitable, however, the concentration function needs more computational calculation.

In this study, advection process is considered more in the particle transport simulation than dispersion; the particle is simulated in the steady-state fluid flow

but not in turbulent vertex generated in the process of perforation; heavy sand particle used in the research and group tracking history is important. Therefore, Eulerian approach is more suitable in this particle transport simulation.

2.2 Principle of particle dispersion and advection

Advection is a common proppants transport phenomenon, particles are carried by the fluid's movement, and bulk transport is a special kind of advection. Generally, steady-state fluid is used in the bulk transport analysis, and the tracking of the bulk particles is the objective of that research. Bulk's travel paths and travel time are computed by the iteration calculation of particles along the streamlines in the fluid.

Compared to advection, dispersion is more complicated and difficult to analyze in the particle simulation. Mixing, spreading and bulk transport are three special processes for particle dispersion. Mixing is the operation of multiple kinds of particles generating into a homogeneous mixture. Spreading is the process of particles moving into new regions where no particles occupied before, simultaneously, particle concentration decreased with the continuation of spreading (Bulk transport also happens in the operation of dispersion). The travel path for specific bulk particles is more similar with advection, the difference is more new regions occupied in the dispersion. All these three types of particle dispersion can happen separately or simultaneously.

By comparing these two operations of particle transportation, Advection is

much close to the real proppants transportation after the perforation area. By applying the Eulerian model to analyze particle advection, many different forces would be considered to generate the travel path every time. These forces could be drag, pressure gradient, virtual mass force, virtual Basset force, Brownian, and body forces. Depending on different factors, such as particle size and concentration, these forces impact on the particle trajectory altogether with different extent.

2.3 Boundary element method

The boundary element method (BEM) is a computational method for solving partial differential equations (PDEs). BEM is widely applied in engineering and science areas, such as fluid mechanics, fracture mechanics, electromagnetic. This method can be employed when the physical problem can be formulated as integral equations, and these equations could be an accurate solution for the PDEs. Meanwhile, BEM is applied in the linear homogeneous media problems for which Green's functions could be solved.

As with the well-known finite element method (EFM) and finite difference method (FDM), BEM is in the same topic of applied mathematics. Nevertheless, the potential advantages of the BEM could be more considerable than the other two numerical methods. For example, when BEM is applicable, the result is often used easily and the computational cost is much lower than the other methods. Because the boundaries of the domain of the PDEs could be subdivided to produce a surface and boundary mesh, by contrast, EFM and FDM requires the whole domain's

discretization. For example, a three-dimensional governing equation could be transformed into one dimension by applying BEM method, EFM and FDM method need the three-dimensional equation discretization. Thus, BEM is more efficient than the other two methods in terms of computational calculation.

In this study, the BEM approach is applied to solve fracture propagation in the fluid and fracture mechanics. Rock is treated by hydraulic pressure with proppants transportation in the energized fluid by linear elastic fracture mechanics (LEFM) theory, fracture propagation and proppants distribution are analyzed in the simulation.

2.4 Linear elastic fracture mechanics

Fracture mechanics is the study of fracture propagation by applying analytical solid mechanics, this method computes the external force on a crack and the materiel's resistance to that force, and experimental solid mechanics of that material is the necessity before studying the fracture characters. Linear elastic fracture mechanics (LEFM) assumes that material is linear elastic, and this theory was developed in 1920. Griffith's criterion and Irwin's modification are significantly important in the foundation and development for the fracture mechanics, and then a powerful criteria is established for the predication of crack propagation.

The energy rate approach and the stress intensity approach are two alternative methods to study the fracture mechanics. Griffith suggested the energy

rate approach based not only on the potential energy of the external loads and the stored elastic strain energy in the material, but also on the surface energy of the material. Irwin modified the version of Griffith's energy criterion by introducing the critical energy release rate Gc, a new calculation method of energy available for fracture in the formation of the stress intensity factor KI.

Mode I fracture, Mode II fracture and Mode III fracture are three generally applicable modes for analyzing crack propagation. Take Mode I fracture as an example, In terms of energy release rate, G is computed as energy release per unit increase crack, if G<Gc, the crack does not happen, conversely, the crack propagates, in the case of G=Gc, the equilibrium is obtained; in terms of stress intensity factor, stresses at the tip of the crack are (three charts),

$$K_I = \sigma\sqrt{a} \cdot f(g) \quad (1)$$

The above equation indicates that stress intensity factor is linearly related to stress and the square root of a characteristic length.

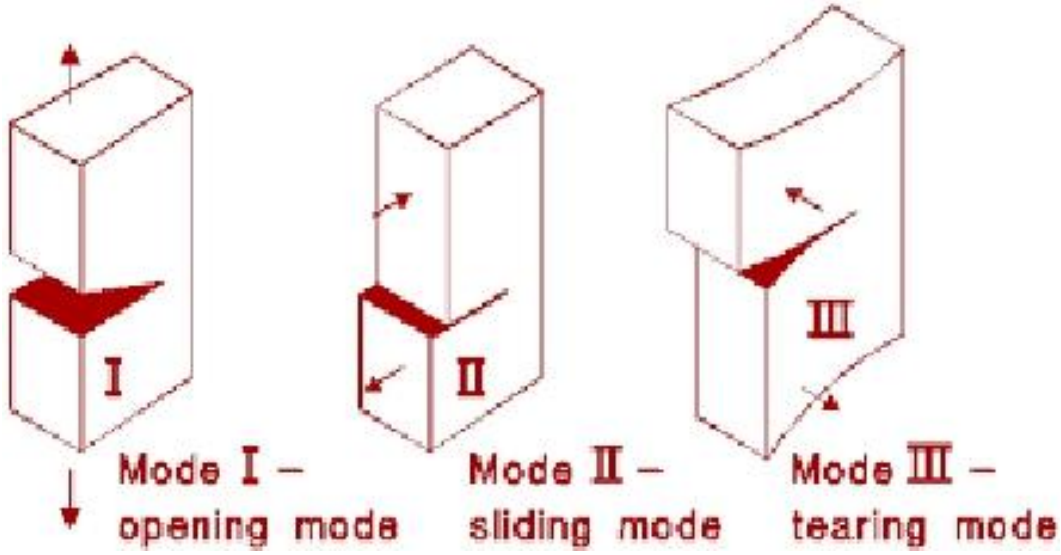

Figure 2.1 Three fracture models, https://en.wikipedia.org.

In the circumstance of LEFM, the stress intensity approach is more applicable than the energy rate approach, since the stress intensity factor could be extracted from stress analysis of rock material by employing the boundary element method.

2.5 Fracture propagation model

Since 1955, Howard and Fast published the first fracture mathematical model to research fracture propagation, two dimensional models, such as Perkins-Kern-Nordgren (PKN) model, Kristonovich-Geertsma-de Klerk (KGD) model, Penny-Shaped model, and different kinds of three-dimensional models are improved significantly with the benefit of the high developing computational simulation technology and microseismic measurement of underground subsurface data.

2.5.1 PKN model

The PKN model solves fracture length and width with a specific height by adding fluid leakoff. The model defines that the energy consumption for the fracture propagation is less than that required for fluid to flow in the fracture, since the influence of fracture toughness is assumed too small to change the fracture distribution. From the aspect of solid mechanics, the fracture height is fixed and is much smaller compared to fracture length, hence, the plane strain would happen in the vertical direction, and the fracture propagation spreads along the horizontal direction. From the aspect of fluid mechanics, the shape of PKN model is ellipse in on dimension channel, and fluid pressure is considered to be constant in each vertical cross section.

2.5.2 KGD model

KGD model is also two-dimensional model for hydraulic fracture research and developed by Khristianovitch and Zheltov (1955), Geertsma and de Klerk (1969). In terms of solid mechanics, the model is assumed that the cross section of fracture is ellipse in the horizontal plane, and each horizontal plane is independent of disfiguration. Moreover, the fracture has certain height, and cross section in the vertical direction is rectangular since along fracture height the width is assumed constant. From the aspect of fluid mechanics, fluid pressure is not constant in the propagation direction and is determined by the flow resistance of the fracture channel, however, the resistance could not be from the upper fracture, because there

is no necessity for fluid to fill the entire fracture length.

2.5.3 Penny-shaped model

Penny-Shaped model defines that the fracture is propagated in a given plane, the cross-section of penny-shaped as it is named is symmetrical with a point where fluid is injected, and constant fluid injection rate and pressure are assumed in the simulation of hydraulic fracture. This model improves the simulation of complex fracturing in shale gas and provides the dimensions of the fracture-network and proppant distribution. However, Penny-Shaped model has two limitations; one is that the model can not solve the fracture network with pre-existing nature fracture; another is the assumption of symmetric elliptical cross-section, because significant asymmetry is normal in the real simulated fracture.

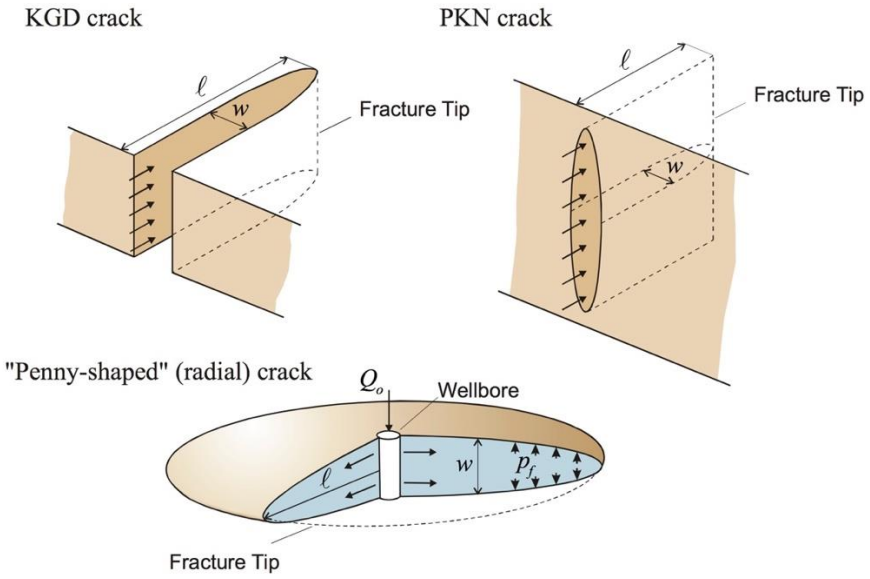

Figure 2.2 Three fracture propagation models. www.cefor.umn.

2.5.4 Pseudo three-dimensional and three-dimensional models

As the advancement of computational technology and geo-mechanical interpretation, simulation of fracture propagation has progressed significantly from 2D model to pseudo three-dimensional model (P3D) and three-dimensional model (3D). P3D model replaces the assumption of constant height from 2D model as a function of position along the fracture and pumping time, and 3D model removes more assumptions from P3D model. Wire-mesh model and unconventional fracture model (UFM) are popular 3D models for hydraulic fracturing simulation. Wire-mesh model could simulate the fracture dimensions and proppant placement in the network. However, there are two limitations in this model; one is that pre-existing natural fractures are not directly connected with the ellipsoidal fracture pattern; another limitation is that the network pattern is symmetric with respect to the injection point and the cross-sectional shape is elliptical, this assumption contradicts the asymmetry and irregular shape of the real micro-seismic date. Comparing of wire-mesh model, UFM improves the ability to simulate interaction with pre-existing natural fracture. However, all natural fractures are vertical with random horizontal angle, because intensive computational time is needed if setting fractures as real natural fracture. Nevertheless, with the integration technologies of reservoir characterization, geo-mechanical modeling, micro-seismic interpretation, and production-simulation tools, the UFM becomes more powerful as a software platform. After all, more real 3D simulation software is acquired as hydraulic fracturing continues to develop.

2.5.5 Comparison among 2D models

PKN, KGD, and Penny-Shaped model are three main two-dimensional models, the following table 2.1 (Xiang, 2011) illustrates the comparison of these three types of 2D mathematic hydraulic fracture models.

Table 2.1 Comparison Between Traditional 2D Hydraulic Fracture Models

Model	Assumptions	Shape	Application
PKN	Fixed Height, Plain Strain in vertical	Elliptical Cross	Length »Height
KGD	Fixed Height, Plain Strain in horizontal	Rectangle Cross	Length «Height
Radial	Propagate in a given plane, Symmetrical to	Circular Cross	Radial

2.5.6 Comparison between two-dimensional model and three-dimensional model

The 2D fracture model are practical mathematical simulation with simplified assumptions. However, the simplified assumptions could have limitations when the cross section is not specific of fixed height or penny-shaped. Pseudo-3D model could remove the assumption of constant height instead of a function of position along the fracture and pumping time. Besides that, vertical fluid flow is added into consideration in the P3D model and it replaced only one direction of fluid flow in the 2D models. Unconventional fracture model further adds the influence of pre-

existing natural fracture for the fracture network. Therefore, the more real 3D model is, the more assumptions should be removed from the 2D model; arbitrary cross-session shape, fluid flow and natural fracture are simulated to the actual occurrence in the process of hydraulic fracturing.

2.6 Particle Reynolds number and regime definition for different forces

When analyzing particle motion in the multiphase flow, particle Reynolds number is the determining factor for classification regimes. Stokes regime, Newtonian regime, and transitional regime are three typical regimes and dominated by viscous forces, inertial forces, a combination of these two forces respectively. These forces could be classified into three types.

The first type of forces includes inertial force, gravity and buoyancy, they are not caused by the relative motion of solid and fluid. The second type of forces are contributed by the relative motion of solid and fluid, they are parallel to the motion direction and comprised of the friction between the phases, virtual mass, and basset force. The last type of forces is created by the relative motion as well but perpendicular to the motion direction; they are lift forces, such as Magnus force and Saffman force.

These forces cumulatively impact the particle motion; which forces are more dominating than others are not only dependent on the regime classified by particle Reynolds number, but also impacted by the size and density of the particle.

The particle Reynolds number equation could be the following equation

$$Re_p = \frac{dV_s}{v_c} \quad (2)$$

Where d is the diameter of particle, V_s is particle velocity comparing to fluid, and v_c is the kinematic viscosity.

2.6.1 The first type of forces

Inertial force, gravity and buoyancy are the first type of forces, they are not caused by the relative motion of solid and fluid.

The inertial force equation

$$F_i = -\frac{\pi}{6} d^3 \rho_P \frac{du_{Py}}{dt} \quad (3)$$

The gravity equation

$$F_g = \frac{\pi}{6} d^3 \rho_P g \quad (4)$$

The buoyancy equation

$$F_b = -\frac{\pi}{6} d^3 \rho_c g \quad (5)$$

Where d is the diameter of particle, ρ_p is the density of particle, ρ_c is the density of continuum fluid, g is gravitational acceleration.

2.6.2 The second type of forces

The second type of forces are contributed by the relative motion of solid and fluid, they are parallel to the motion direction and comprised of the friction between the phases, virtual mass, and Basset force.

The friction between the phases, virtual mass and Basset force are parallel to the motion direction and caused by the relative motion of particle and the

multiphase flow.

The friction between the phases is also named drag force, the equation is as (6),

$$F_f = \frac{\pi}{8} C_D d^2 \rho_c |u_{cy} - u_{py}|(u_{cy} - u_{py}) \quad (6)$$

where C_D is the drag coefficient, ρ_c is the density of the carrier fluid, d is the particle diameter, $|u_i - v_i|$ and $(u_i - v_i)$ are absolute and relative differential velocity of fluid and particle.

In different range of particle Reynolds number, cd has different form. For larger particles or particle Reynolds number is larger than 1000, in this range inertial forces are dominate effect than viscous forces, and this region is known as the Newtonian Region, C_D is approximately constant and equal as 0.44. By contrast, for very small particles or particle Reynolds number is less than 1, viscous forces are more effective than inertial forces. In this situation, the C_D takes the form as (2-14). For particles diameter interposed between these above situations or particle Reynolds number is less than 1000 but larger than 1, C_D comes from the following equation (7), both inertial force and viscous force need to be considered in this range.

Virtual mass is the additional inertial force since particle acceleration or deceleration has to move with surrounding fluid as it moves through the carrier fluid. In other words, this could be modeled as the particle with extra volume of fluid as a new object, and the extra fluid is the reason of the additional mass

force. The formulation of the virtual force is taken as:

$$F_a = -\frac{\pi}{12} d^3 \rho_c \left(\frac{du_{py}}{dt} - \frac{du_{cy}}{dt} \right) \quad (7)$$

Basset force has the same reason of particles acceleration or deceleration in the fluid, the difference is that basset force is caused by viscous effects due to lagging boundary layer formed by the relative motion of particle and fluid. Thus, the Basset force lag behind the changing velocity of particles, and equation of this force is seen as:

$$F_{Basset,i} = \frac{3}{2} d^2 \sqrt{\pi \rho_c \mu_c} \int_0^t \frac{\frac{dy}{dt'}(u_i - v_i)}{\sqrt{t - t'}} dt' \quad (8)$$

Generally, when ρ_c / ρ_p ⊔ 0.001, the virtual mass force and Basset force become ineligible.

2.6.3 The third type of forces

The last type of forces is created by the relative motion as well but perpendicular to the motion direction; they are lift forces, Magnus force and Saffman force.

The Saffman Lift Force and the Magnus Lift Force are two typical lift forces determining the lift forces of a particle within a continuum multiphase flow and perpendicular to the motion direction. Depending on the scale of particle size, these two lift forces are applied into different particle Reynolds number range.

For the Saffman force, the equation is:

$$F_{saff} = 0.161 \mu_c d |u_i - v_i| \sqrt{Re_g} \quad (9)$$

where μ_c is the pumping fluid dynamic viscosity, d is the particle diameter, $|u_i - v_i|$ is the absolute differential velocity between fluid and particle, and $Re_g$is the shear Reynolds number formulated as:

$$Re_g = \frac{d^2 du}{v_c dy} \tag{10}$$

The Saffman force is a shear lift force originated from the inertial effects in the viscous flow and generated by different pressure forcing on a particle because of its velocity gradient. However, this force is insignificant when the particle Reynolds number is more than 1.

In the case of the Magnus lift force, the equation is:

$$F_{mag} = \frac{\pi}{8} d^3 \rho_c w_d (v - u) \tag{11}$$

where ρ_C is the density of carrier fluid, $\omega_d$is the angular velocity for particle, and $(v - u)$ is the differential velocity of particle and pumping fluid. The Magnus force is generally applied for a spinning ball or a cylinder turning away from its main trajectory. For particle, diameter ranging from millimeter scale is the observing object for the Magnus force. Thus, the Magnus force is applied for large particles and the particle Reynolds number should be more than 1000.

2.6.4 Other force: Brownian force

Apart from the above three types of forces, Brownian force exists when particles transport and interact with atoms and molecules in the fluid. Particles impart and export kinetic energy from that atoms and molecules. Moreover, the

interaction is a random collision and a discrete interaction of particle to phase.

The Brownian force influences the motion of particle by exchanging kinetic energy with fluid atoms and molecules. However, simulating this process is computational intensive in the atom and molecule level, and this atom and molecule level is not the same level as the other forces discussed above. Thus, the Brownian force is negligible even though it really exists.

2.6.5 The comprehensive particle forces equation

Particle is simplified as sphere, vertical down and up are defined as positive and negative direction for particle as rising up and settling down. Depending on the specific three types of particle forces analyzed above, the comprehensive particle force equation could be deduced as follows:

In the y direction:

$$\frac{\pi}{3}d^3\rho_p\frac{du_{py}}{dt}=\frac{\pi}{6}d^3(\rho_p-\rho_c)g+\frac{\pi}{8}C_Dd^2\rho_c|u_{cy}-u_{py}|(u_{cy}-u_{py})$$
$$-\frac{\pi}{12}d^3\rho_c(\frac{du_{py}}{dt}-\frac{du_{cy}}{dt}) \quad (12)$$

In the x direction

$$\frac{\pi}{3}d^3\rho_p\frac{du_{px}}{dt}=\frac{\pi}{8}C_Dd^2\rho_c|u_{cx}-u_{px}|(u_{cx}-u_{px})-\frac{\pi}{12}d^3\rho_c(\frac{du_{px}}{dt}-\frac{du_{cx}}{dt}) \quad (13)$$

2.7 Methodology of fluid flow equations

Numerical solution of fluid flow in the fractures is required of modeling flow by governing equations. On the hypothesis of single phase, Newtonian, and constant density fluid, the basic governing equations are described as mass and

momentum conservation. In the scalar form for 3 dimensional fluid flow, those two equations could be written as following:

$$\frac{\partial u}{\partial x}+\frac{\partial v}{\partial y}+\frac{\partial w}{\partial z}=0 \tag{14-1}$$

$$\rho\left(\frac{\partial u}{\partial t}+u\frac{\partial u}{\partial x}+v\frac{\partial u}{\partial y}+w\frac{\partial u}{\partial z}\right)=-\frac{\partial P}{\partial x}+\mu(\frac{\partial^2 u}{\partial x^2}+\frac{\partial^2 u}{\partial y^2}+\frac{\partial^2 u}{\partial z^2}) \tag{14-2}$$

$$\rho\left(\frac{\partial v}{\partial t}+u\frac{\partial v}{\partial x}+v\frac{\partial v}{\partial y}+w\frac{\partial v}{\partial z}\right)=-\frac{\partial P}{\partial y}+\mu(\frac{\partial^2 v}{\partial x^2}+\frac{\partial^2 v}{\partial y^2}+\frac{\partial^2 v}{\partial z^2}) \tag{14-3}$$

$$\rho\left(\frac{\partial w}{\partial t}+u\frac{\partial w}{\partial x}+v\frac{\partial w}{\partial y}+w\frac{\partial w}{\partial z}\right)=-\frac{\partial P}{\partial z}+\mu(\frac{\partial^2 w}{\partial x^2}+\frac{\partial^2 w}{\partial y^2}+\frac{\partial^2 w}{\partial z^2}) \tag{14-4}$$

Where u, v, w is x, y, z direction of velocity. Equation (14-1) is Continuity Equation, and Equation 14-(2-4) are known as Navier-Stokes Equation.

The Navier-Stokes equation also could be expressed as vector form,

$$\rho(\mathrm{u}\cdot\nabla)\mathrm{u}=-\nabla P+\mu\nabla^2 u \tag{15}$$

This nonlinear partial differential equation has no general analytical and numerical solution based on the incompressible and steady-state assumption. In the case of modeling subsurface flow, advective term is small enough to be neglected. After dropping out the advective term, a much simpler form could be solved numerically and expressed as the following:

$$\nabla P=\mu\nabla^2 u \tag{16}$$

The simpler Navier-Stokes equation is Stokes equation, and could be valid governing equation for simulating fluid in fractures when the fracture walls are approximate parallel, the speed of flow is slow enough to be seen as laminar

fluid. In other words, the effect of advection term vanishes at low speed between the relative parallel fracture walls.

2.8 Parallel plate model and particle assumptions

Parallel plate model might be the simplest model for fluid flowing through a fracture and also a numerical model for hydraulic conductivity calculation. The model assumes the fracture walls are two smooth, parallel plates. The two plates are separated by an aperture 2b and steady-stated laminar fluid flows between the plates. This model creates a uniform pressure gradient and unidirectional flow. The fluid is in the x-direction, and the velocity exists only in the x direction.

The numerical solutions for velocity and flow rate are expressed in the following equations:

$$U_x(y) = -\frac{1}{2\mu} \cdot \frac{dp}{dx}(b^2 - y^2) \tag{17}$$

$$Q(x) = -\frac{b^3}{12\mu}\frac{dp}{dx} \tag{18}$$

Where p is the continuum fluid pressure, μ is the viscosity of the fluid, 2b is the aperture of the fracture. Because flow rate equation includes the factor of b^3, the flow rate is also called as "cubic law".

When particles are transported in the fluid and properly fitted into the parallel plate model, four assumptions for particle should be formulated by the Stokes law. Particles are smooth surface, spherical form, homogeneous material and no interference with each other.

2.9 Mass conservation

Based on the continuum theory, two mass conservative equations about particle and fluid transport are derived and expressed as the following (19) (20),

$$\frac{\partial(C\cdot w\cdot u_{px})}{\partial x}+\frac{\partial(C\cdot w\cdot u_{py})}{\partial y}+\frac{\partial(C\cdot w)}{\partial t}=0 \tag{19}$$

$$\frac{\partial[(1-C)\cdot w\cdot u_{cx}]}{\partial x}+\frac{\partial[(1-C)\cdot w\cdot u_{cy}]}{\partial y}+\frac{\partial[(1-C)\cdot w]}{\partial t}=0 \tag{20}$$

Where: C- sand ratio dimensionless, w - width of fracture, p_c- pressure in fluid, u_{cx}- horizontal velocity of fracturing fluid, m/s, u_{px}-horizontal velocity of particle, m/s.

Chapter 3

Modeling Fluid-Driven Sand Insertion

3.1 General description

Hydraulic fracturing is generally divided into two stages. The first stage is of pumping energized water without proppant material to create fracture and then water is drawn back to the surface ground. The next stage is of pumping slickwater consisted of water and sand with additional chemical to keep the fracture open by the function of sand when water is flushed back to the ground. Sand distribution influenced by the function of ground operation, fluid and rock mechanics is the main objective of this studying. Eight theories including particle tracking, dispersion and advection, boundary element method (BEM), linear elastic fracture mechanics (LEFM), fracture propagation model, particle Reynolds number and regime definition for different forces, fluid flow equations and mass conservation are applied for simulating sand distribution.

For sand, particle tracking, dispersion and advection, particle Reynolds number and regime definition for different forces are related for studying sand's force and motion. Simulation result is defined in terms of a concentration field, the Eulerian model would be more suitable for analyzing the particle as a continuum phase. As a continuum phase, advection is more practical for tracing sand's path and travel time as bulk transport in the steady-state fluid. Since particle Reynolds is larger than 1 and less than 1000, combination of viscous forces and inertial forces

are considered in the transitional regime when sand and fluid are transported in the fracture.

For fluid, the flow is governed by Stokes equation. Simulation of fluid in the approximate parallel fractures, lubrication theory is valid when flow speed is slow enough to be seen as laminar fluid.

For rock mechanics, penny-shaped model and LEFM are applied to model and propagate fracture. The cross-section of penny-shaped model is symmetrical with a point where fluid is injected, and constant fluid injection rate Q_O and pressure P_f are assumed in the simulation of hydraulic fracture (figure 3.1), in the modeling half cross-section of penny-shaped model is applied; LEFM assumes that material is linear elastic, and the stress intensity approach is more applicable than the energy rate approach, since the stress intensity factor could be extracted from stress analysis of rock material by employing the boundary element method.

For the whole model, BEM are applied to computationally solve fracture propagation, fluid and sand distribution, two mass conservative equations about particle and fluid transportation are derived based on the continuum theory.

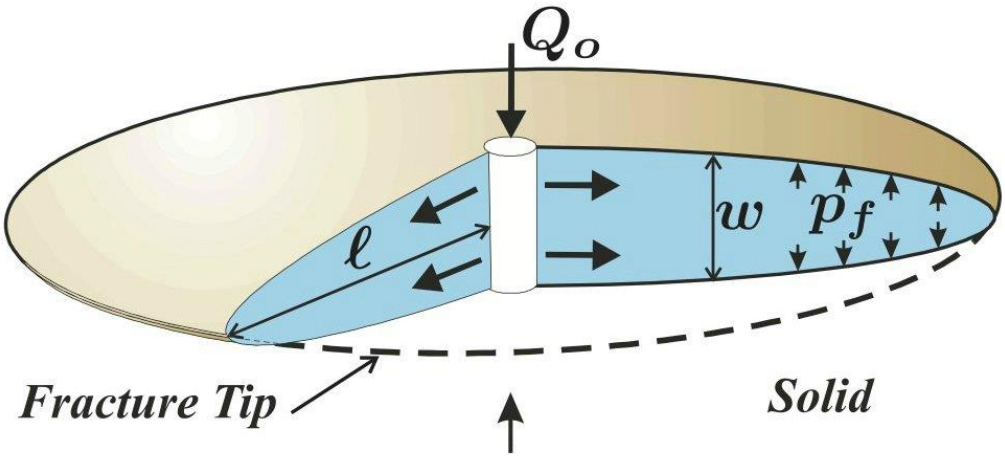

Figure 3.1 Penny-shaped model with injection Q_o and P_f, www.cefor.umn.

3.2 Two relevant numbers about sand distribution in hydraulic fracture

Reynolds number (Re) and Péclet number (Pe) are two related number for sand motion in the hydraulic fracture. Re is defined as the ratio of inertial forces to viscous forces for particle sand in the energized fluid. Pe is identified as the ratio of advective transport rate to diffusive transport rate for sand distribution.

When analyzing particle motion in the multiphase flow, particle Reynolds number is the determining factor for classification regimes. Stokes regime, Newtonian regime, and transitional regime are three typical regimes and dominated by viscous forces, inertial forces, a combination of these two forces respectively. These forces cumulatively impact on the particle motion, however, the forces more dominating than others are not only dependent on the regime classified by particle Reynolds number, but also impacted by the size and density of the particle. The

particle Reynolds number equation could be the following equation:

$$Re_p = \frac{dV_s}{v_c}$$

Where d is the sand diameter, V_s is sand velocity in the fluid, and v_c is the kinematic viscosity for fluid, and expressed as $v_c = \frac{\mu}{\rho}$.

According to Detwiler and Rajaram (2000), a combination of physical experiments and computational simulation is applied to test a theoretical model. In the model, an important coefficient D_L in terms of the effective longitudinal dispersion is written as a sum of the contributions of the three dispersive mechanisms.

Three distinct dispersion regimes are categorized by P$\acute{e}$clet number. For $Pe \ll 1$, this region is molecular diffusion and $D_L \propto Pe^0$; for intermediate Pe, macrodispersion is predominant and $D_L \propto Pe$; for large Pe, Taylor dispersion dominates and $D_L \propto Pe^2$.

P$\acute{e}$clet number $Pe = V(b)/D_m$, where V is the mean particle velocity, b is the mean aperture, and D_m is the molecular diffusion coefficient.

For Taylor dispersion, D_L could be expressed as:

$$D_{L,Taylor} = \frac{V^2 b^2}{210 D_m}$$

A straightforward and simplified advection with minor diversion modeling approach is more practical in the simulation of sand distribution in the hydraulic fracturing. The main objective of this research is to obtain basic knowledge about

sand transport phenomena in the fracture with mechanical shear displacement, instead of complicated transport simulation; due to the diffusion of particles in the hydraulic fracture, the random dispersion, the retardation mechanisms are not necessary to be considered. Moreover, most dispersion occurs at fracture entrance area when plug-and-perf completion with different perforation phasing, and advection is more dominated when particles are carried by energized fluid after the entrance area. Lastly, intense computational cost is also taken into account when calculating the solution of dispersion.

3.3 Governing equation for sand insertion in the single crack geometry

In the homogeneous, isotropic, linear elastic and impermeable rock Ω, existed fracture Γ is driven by a single two-dimensional plan strain slickwater Q_0, see Figure 3.1. Tractions τ, displacement Γ_u and fracture face Γ_c are imposed for the boundary domain Γ_f.

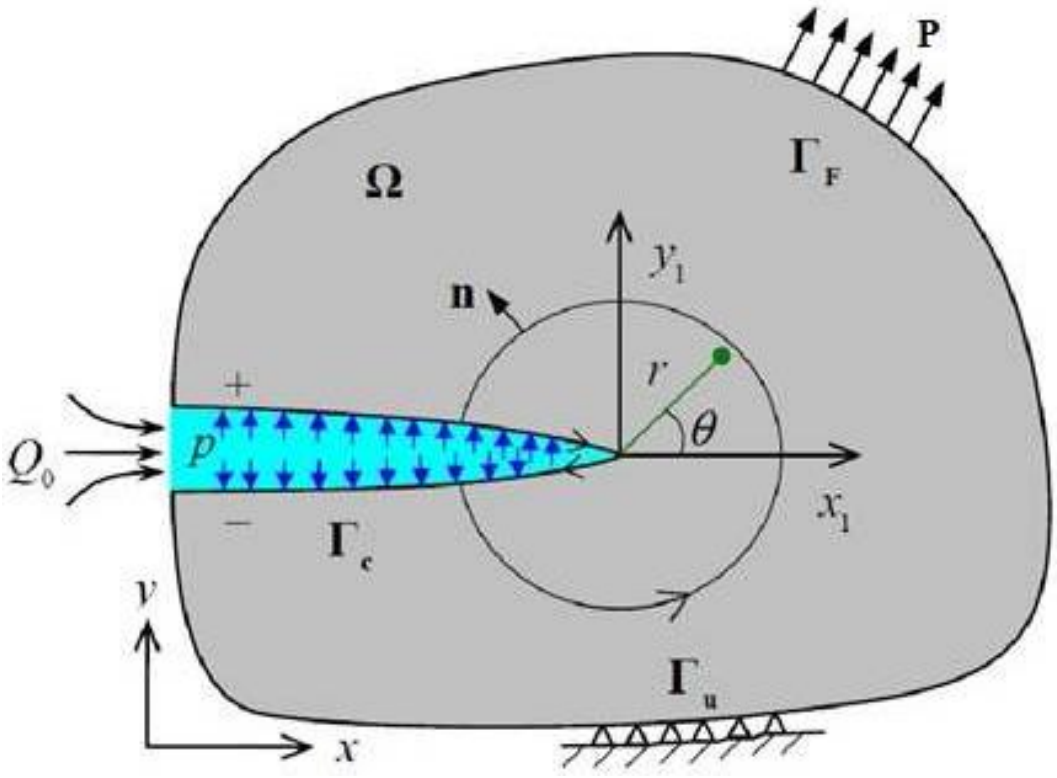

Figure 3.2 A homogenous, isotropic, linearly elastic body Ω with piecewise smooth boundary Γ in equilibrium. www.intechopen.com

Incompressible Newtonian slickwater at flow rate Q is injected into the homogeneous, isotropic, linear elastic and impermeable rock. For this study, sand distribution is determined by analyzing the mutual mechanics influence of sand, fluid and rock. The normal and shear stress, σ and τ, are expressed by fluid pressure P and displacement u as an equilibrium equation:

$$\sigma_{i,j} = -P\sigma_{i,j} + \mu(u_{i,j} + u_{j,i}) \tag{21}$$

where P is the stress tensor component in i and j direction, μ is the dynamic

viscosity, u is the displacement component in the i and j direction. The traction is at the outer boundary, equal magnitude but opposite direction and is given as,

$$\sigma \cdot \mathrm{n} = \hat{t} \tag{22}$$

Hence, σ and τ could be expressed as the following:

$$\sigma_x = -P \tag{23}$$

$$\sigma_y = -P + \mu \frac{\dot{w}}{w} \tag{24}$$

$$\tau^+ = \mu(-4\frac{V_m}{w} + \frac{\dot{w}}{w}) \tag{25}$$

$$\tau^- = \mu(4\frac{V_m}{w} + \frac{\dot{w}}{w}) \tag{26}$$

Equation 23 and 24 are the stresses acting in the x and y direction inside the fracture. Equation 25 and 26 are shear stress acting on the fracture surface, equal in magnitude but opposite direction. Where V_m is the velocity of the fluid at the entrance point of fracture, w is the fracture opening at that point, assuming parabolic profile for fluid and sand (figure 3.3), the velocity equation is expressed by:

$$V = V_m\left(1 - 4\frac{y^2}{w^2}\right) \tag{27}$$

$$V_S = V_{ms}\left(1 - 4\frac{y^2}{w^2}\right) \tag{28}$$

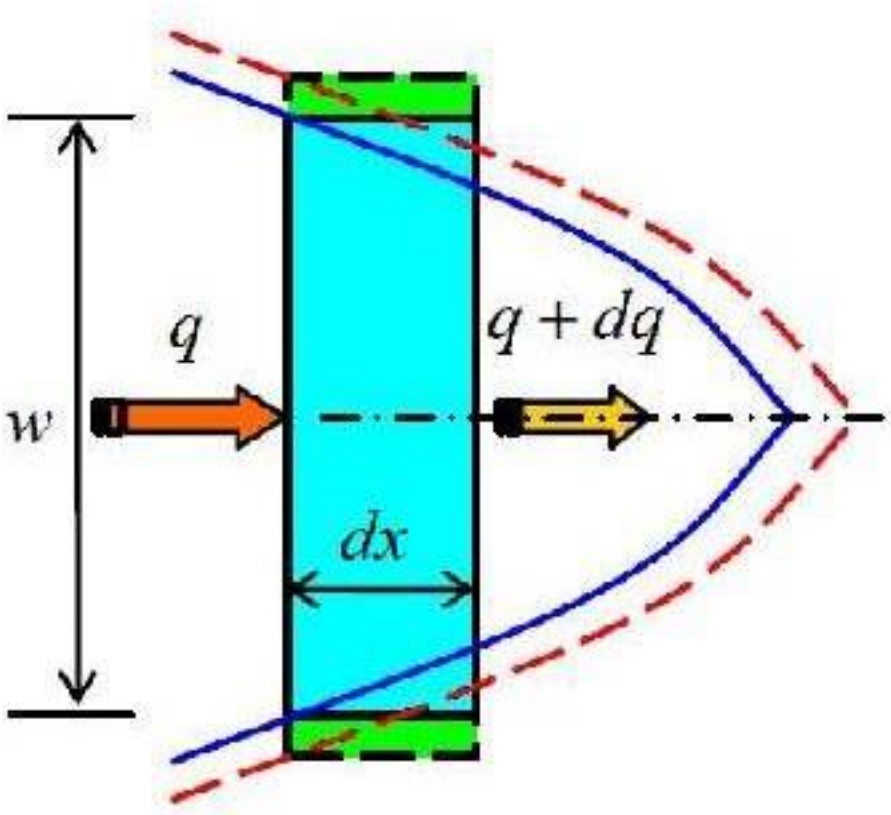

Figure 3.3 Parabolic profile for fluid or sand. http://www.intechopen.com

The fluid velocity inside the crack domain, V_m and V_{ms} are vertex points velocities for fluid and sand at the inlet area. Fluid and sand flow rate are integrated the velocity profile over the opening of the crack, and are expressed as:

$$Q = \int_{\frac{-w}{2}}^{\frac{w}{2}} V_x dx = \frac{2}{3} V_m w \tag{29}$$

$$Q_S = \int_{\frac{-w}{2}}^{\frac{w}{2}} V_{xs} dx = \frac{2}{3} V_{sm} w \tag{30}$$

Assuming impermeable solid rock, the leak-off is negligible and fluid injected into the fracture consists with a constant flow rate Q,

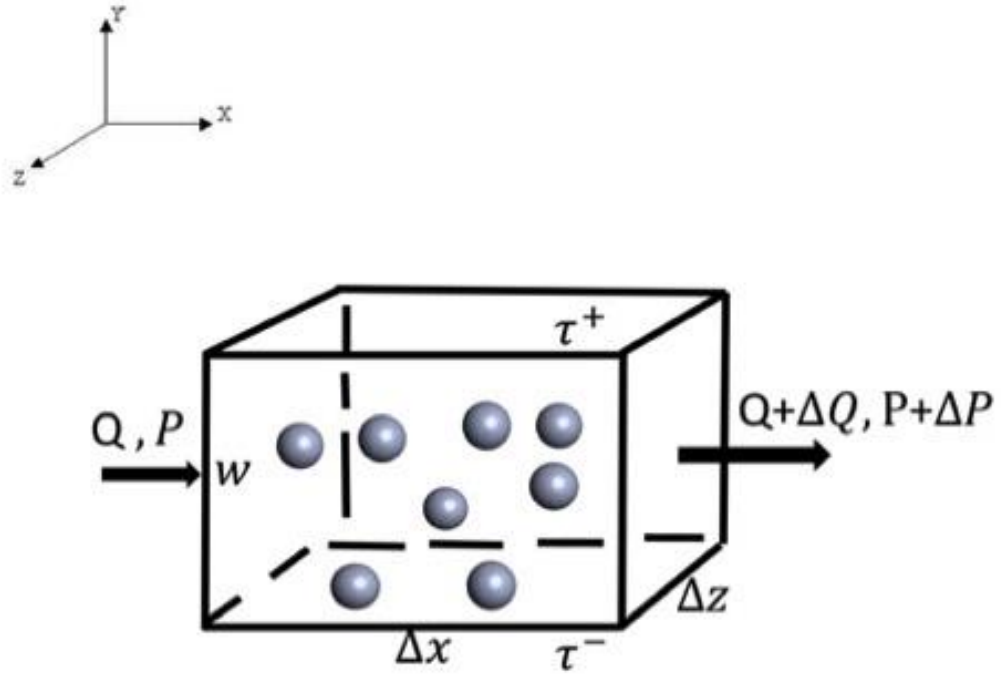

Figure 3.4 Model of sand transportation between the fracture wall

Figure 3.4 is a unit controlling volume of the fluid with sand pumped in the fracture, assuming the size is $\Delta x, w, \Delta z$, C_s is defined as the number of the sand in that unit volume, and P is presumed as only function of x. Only drag force is considered since the interaction between fluid and sand, the equation for a sand is given by:

$$f_d = 6\pi\mu a(V - V_s) \tag{31}$$

Where a is the diameter of sand, $V - V_s$ is the relative velocity of fluid and sand.

Based on the above hypothesizes and definitions, the equilibrium equation about fluid is given by

$$\rho\Delta x\Delta y\Delta z\dot{V} = -\Delta P\Delta y\Delta z + \Delta\tau\Delta x\Delta z - C_s\Delta x\Delta y\Delta z f_d \quad (32)$$

Integration of that equation over the w fracture width could written as:

$$\int_{\frac{-w}{2}}^{\frac{w}{2}} \rho(1-4\frac{y^2}{w^2})\dot{V_m}d =$$

$$-\Delta P\Delta \mathrm{y} + \Delta\tau\Delta \mathrm{x} - \int_{\frac{-w}{2}}^{\frac{w}{2}} C_s 6\pi\mu a(V_m - V_{sm})(1-4\frac{y^2}{w^2})dy \quad (33)$$

Then with the equations 25, 26, 29, 30 and substitution, the fluid equation could be simplified as below:

$$\rho\dot{Q} = -\frac{3}{2}P_{,x} - 12\frac{\mu Q}{w^2} - C_s 6\pi\mu a(Q - Q_S) \quad (34)$$

Similarly, the equilibrium equation about sand is given by:

$$m_s C_s\Delta x\Delta y\Delta z\dot{V_s} = -\Delta P_s\Delta y\Delta z + C_s\Delta x\Delta y\Delta z f_d \quad (35)$$

and then integration over the width of the fracture:

$$\int_{\frac{-w}{2}}^{\frac{w}{2}} m_s C_s(1-4\frac{y^2}{w^2})\dot{V_{sm}}dy \quad =$$

$$-\Delta P_s\Delta \mathrm{y}\Delta \mathrm{z} + \int_{\frac{-w}{2}}^{\frac{w}{2}} C_s 6\pi\mu a(V_m - V_{sm})(1-4\frac{y^2}{w^2})dy \quad (36)$$

$$m_s C_s\dot{Q_s} = -\left(PC_s\frac{4}{3}\pi a^3\right)_{,x} + C_s 6\pi\mu a(Q - Q_S) \quad (37)$$

$$m_s C_s\dot{V_S} = -P_{s,x} + C_s f_d \quad (38)$$

Where P_s is the fluid pressure for sand, could be formulated as:

$$P_s = C_s\frac{4}{3}\pi a^3 P \quad (39)$$

The mass conservation equation about fluid is given by:

$$\Delta Q \Delta t \Delta z = -\Delta w \Delta x \Delta z \tag{40}$$

$$\frac{\Delta Q}{\Delta x} = -\frac{\Delta w}{\Delta t} \tag{41}$$

$$Q_{,X} + \dot{w} = 0 \tag{42}$$

The mass conservation equation about sand is given by:

$$\Delta Q_s \Delta t \Delta z = -\Delta C_s w \Delta x \Delta z \tag{43}$$

$$\frac{\Delta Q_s}{\Delta x} = -\frac{w \Delta C_s}{\Delta t} \tag{44}$$

$$Q_{s,x} + w\dot{C}_s = 0 \tag{45}$$

Considering of sand diversion and advection, the equation is written as

$$Q_x = -DC_{s,x} + C_s V_{s,x} \tag{46}$$

$$\dot{C}_s = -\dot{Q}_x = DC_{s,xx} - C_s V_{s,xx} \tag{47}$$

Where D is the diffusion constant and defined by kinetic theory.

For crack propagation, fracture is cracked by $w_n$when energized fluid with pressure P is injected into the fracture. In the figure 3.3, the displacement discontinuity at the crack tip node is taken as zero, and the crack tip is treated as the last node in a quadratic discontinuous element.

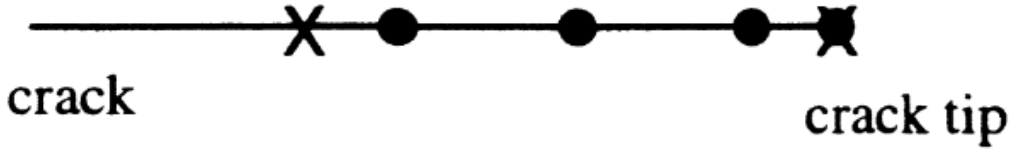

Figure 3.3 Discontinuous crack tip element. Yang, B., and K. Ravi-Chandar. "Evaluation of elastic T-stress by the stress difference method." Engineering Fracture Mechanics 64.5 (1999): 589-605.

All the nodes including the crack tip and the other quadratic discontinuous elements are governed by the regular finite difference polynomial interpolation. (B. Yang, K. Ravi-Chandar, 1999).

Chen (2013) assumed in his paper that small strain and displacement, the kinematic equation includes the strain-displacement relationship, displacement boundary conditions and crack surfaces separation, and seen as:

$$w = V^{+} - V^{-} \tag{48}$$

where $V^{+}$and V^{-} are displacements on two sides of the crack surface. Crack Green function is applied to solve that problem. A similar method is also used in this study. The equation for displacement and traction components is written as:

$$P_i = \oiint V_{ij}^{*} P_j - P_{ij}^{*} V_j dP + \oiint P_{ij}^{*} w_j dP \tag{49}$$

Where P_i is the hydraulic pressure on the ith node, V_{ij}^{*} and P_{ij}^{*} are the Greens functions for displacement and traction. P_j is the normal component of traction in the jth direction, V_j is the displacement in the jth direction, and w_j is the

opening aperture component.

In conclusion, a set of governing equations (34), (38), (42), (47) and (49) are employed to solved three unknown, fracture displacement w, fluid velocity V, sand velocity V_s and sand concentration C_s.

Chapter 4

Simulation and Results

4.1 Numerical algorithm

The numerical algorithm is calculated through an iterative combination of rock propagation, fluid flow and sand distribution. Starting with initial value and boundary conditions, fluid velocity, sand velocity and concentration are calculated until the solution is converged. When the propagation condition $K_{IC} \geq K_I$, the crack propagates to the next node, fluid tip moves to the crack tip, and sand is carried by fluid with velocity V_s and concentration C_s. Otherwise, the fluid tip forwards to the crack tip with velocity V and pressure P, sand probably continues to move forward or already all settle down and deposit along the crack path.

4.1 Numerical results

Before computational calculation, parameters are necessary to be normalized for simplicity and correct result. 10^6 is taken as the normalizing factor for rock elasticity E, the unit is MPa. Fluid normal and tangential pressure are expressed as MPa unit as well. For sand properties, m, Gg, and s is taken as the length, weight and time unit, respectively. For C_s, 1 unit is taken as the sand concentration, and diffusion coefficient is taken as m^2/s. Mpa·s is taken as the unit of fluid viscosity μ. For all length unit of fluid and rock, m is the unit. Lastly, time step unit is taken as s.

After normalizing of units, boundary condition is the next step to be

established for computational simulation. The front view of rock body is square and the perimeter of that square is divided into 5 segments, they are vectors from (0, 0) to (-5, 0), from (-5, 0) to (-5, -10), from (-5, -10) to (5, -10), from (5, -10) to (5, 0), from (5, 0) (0, 0). The crack tip starts from point (0, 0) and propagates almost perpendicular that square front.

Table 4.1 Material Properties and Input Parameters

Parameter		Range
Q	Volumetric Injection Rate	0.01-0.25m^3/s
D	Diffusive coefficient	$10^{-10}m^2/s$
μ	Fluid viscosity	1-5cp
E	Young's Modulus	9-110GPa
K_{IC}	Mode I fracture toughness	0.1-2.7MPa.$m^{1/2}$
a	Sand Radius	0.15-0.25mm
ρ	Sand Density	2.65g/cm^3

With the above normalized units, boundary condition and material properties and parameters in the table 4.1, sand radius, fluid viscosity and pressure would be discussed in the following charts and analysis.

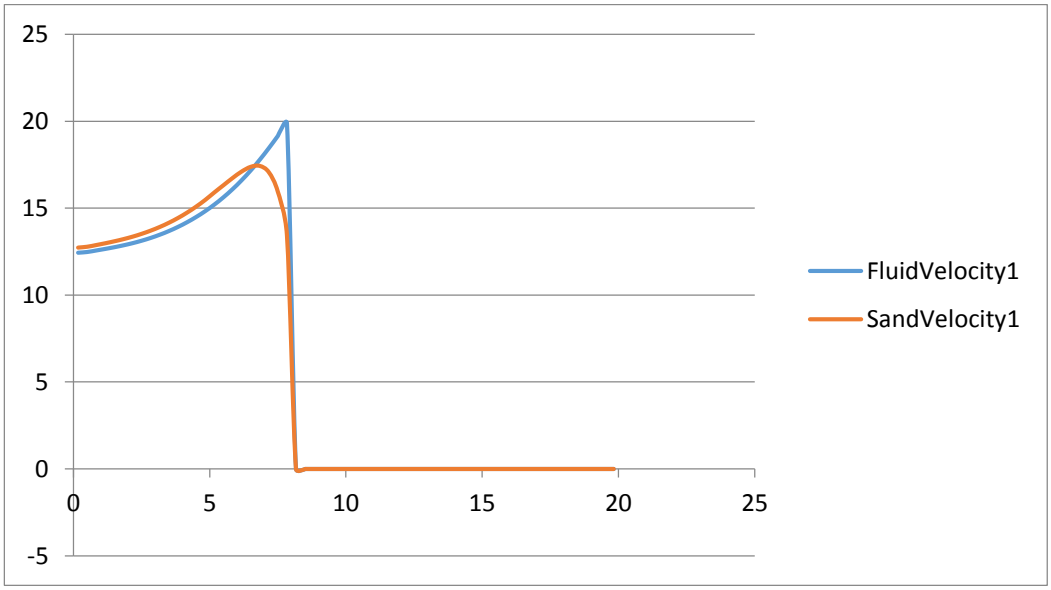

Figure 4.1 Fluid and sand velocity at 1st load case

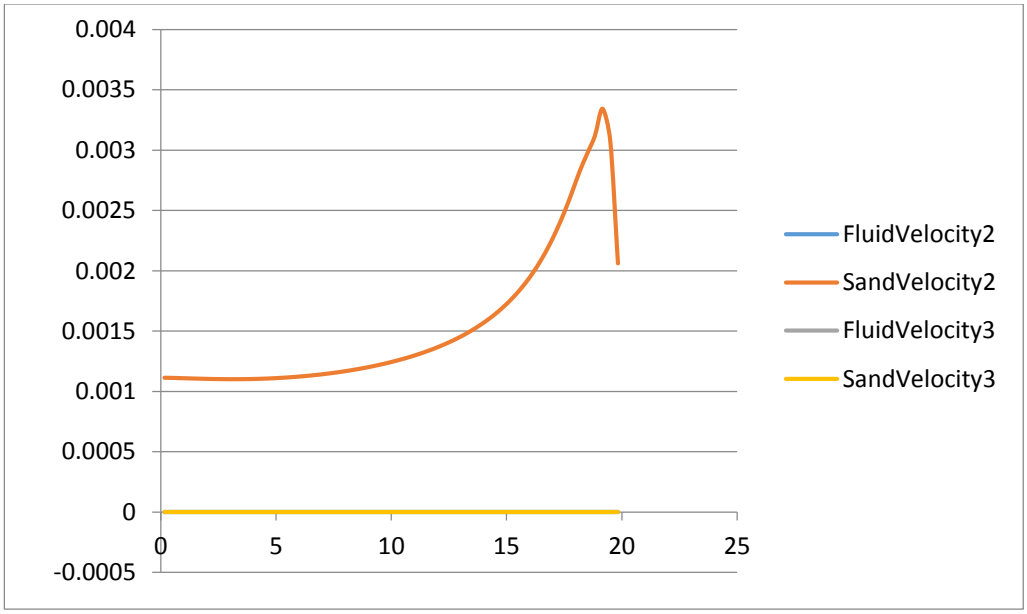

Figure 4.2 Fluid and sand velocity at 6th and 12th load case

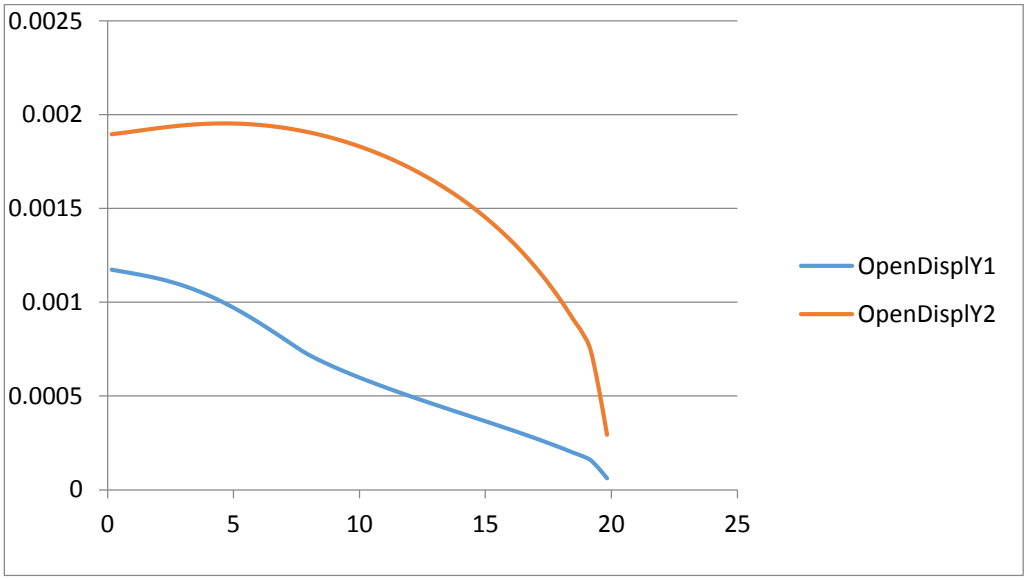

Figure 4.3 Open displacement at Y direction at 1st and 12th load case

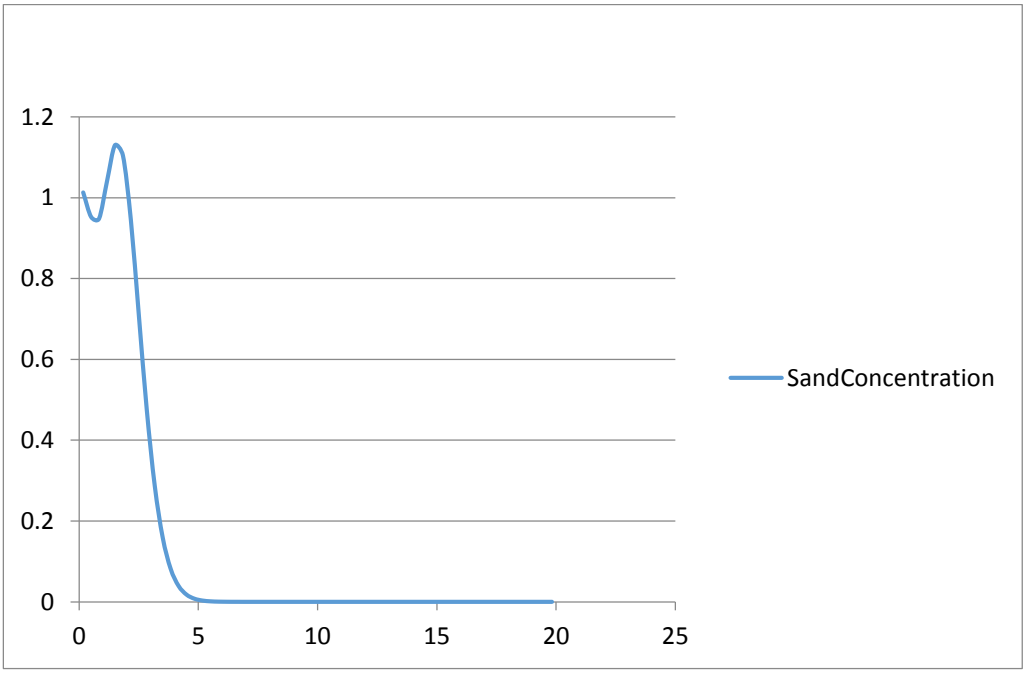

Figure 4.4 Sand concentration at 12th load case

The results are based on the condition of rock elasticity (E) as 30GPa, sand radius as meshed 40/70 0.15mm, sand density 2.65g/cm^3, fluid viscosity as 1cp and fluid pressure 1MPa is applied in the whole 12 load cases. Sand and fluid velocities at 1st, 6th and 12th load cases are studied, fracture displacement in the Y direction are plotted at 1st and 12th load cases, and sand concentration at 12th is pictured.

For the velocities of fluid and sand, initially in the figure 4.1 at 1st load case they are accelerated to the speed more than 10m/s. At the vertex of the energized fluid, fluid velocity is much faster than sand velocity since fluid is the only carrier for sand. By contrast, before that vertex area, sand runs more rapid than fluid because the deceleration for fluid from rock and fluid viscosity is much bigger than sand forced by the mutual function with fluid. At 6th and 12th load case in the figure 4.2, all velocities are closed to zero except sand velocities at 6th load case. At 6th load case, sand still moves forward when fluid already approaches to fracture end, since fluid pressure is not powerful enough to penetrate through the rock and sand become decelerated by the fluid viscosity. Ultimately the velocity of sand and fluid approach to zero.

For the fracture profile, in the figure 4.3 the fracture size at 12th load case increases roughly one time higher than the 1st load case since the function of energized fluid and sand. However, fracture length is identical at the 1st and 12th load case, because fluid pressure is powerless to penetrate through the rock and

transporting sand is the main role of the fluid.

For sand concentration in the figure 4.4, nearly 75% of the fracture was not occupied by sand. By contrast, dense concentration occurs at the first 5 meter of the facture, and peak point where sand concentration is more than 1 unit happens around at the 2.5 m place. Hence, on this condition sands is more concentrated around the perforation area.

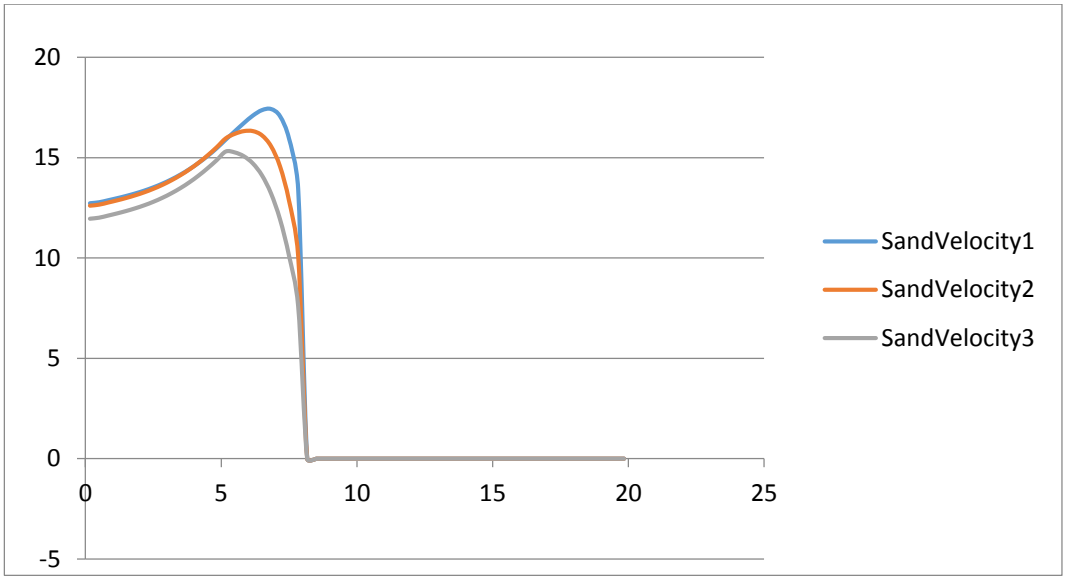

Figure 4.5 Sand velocities at 1st load case when R=0.15, 2, 2.5mm

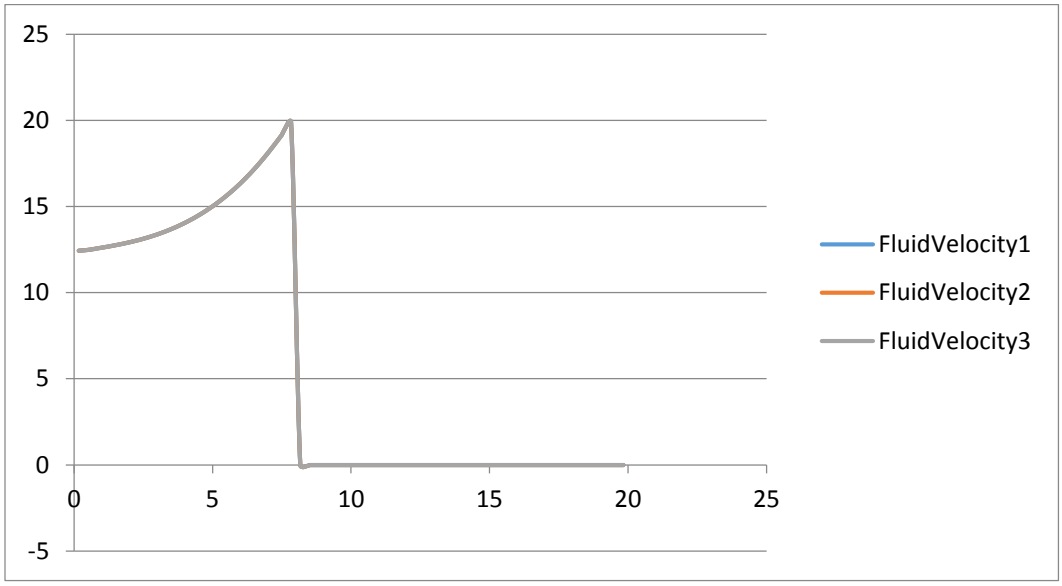

Figure 4.6 Fluid velocities at 1st load case when R=0.15, 2, 2.5mm

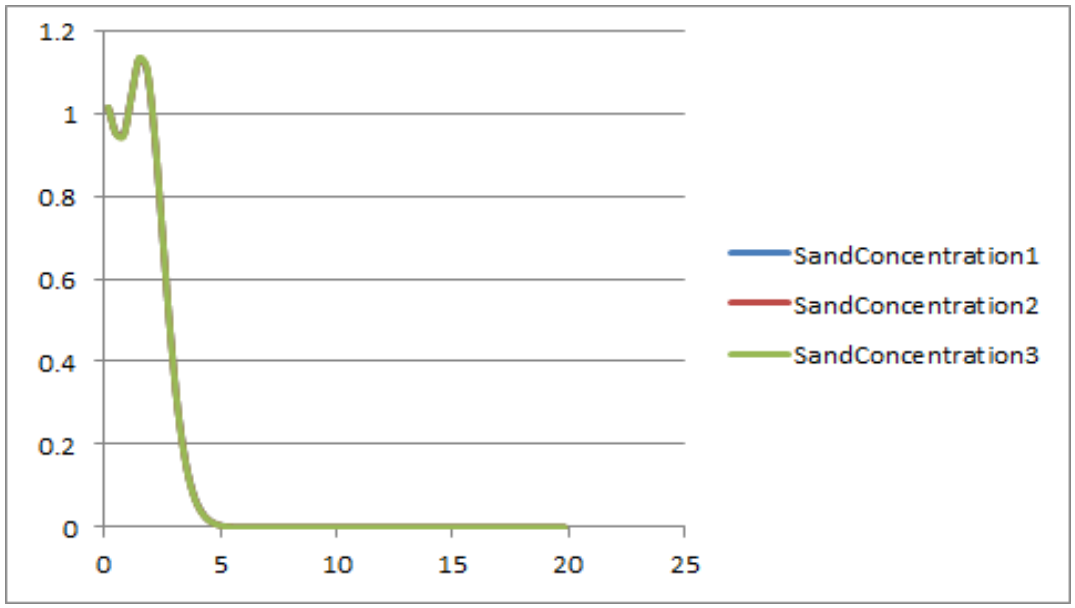

Figure 4.7 Sand concentration at 12th load case when R=0.15, 2, 2.5mm

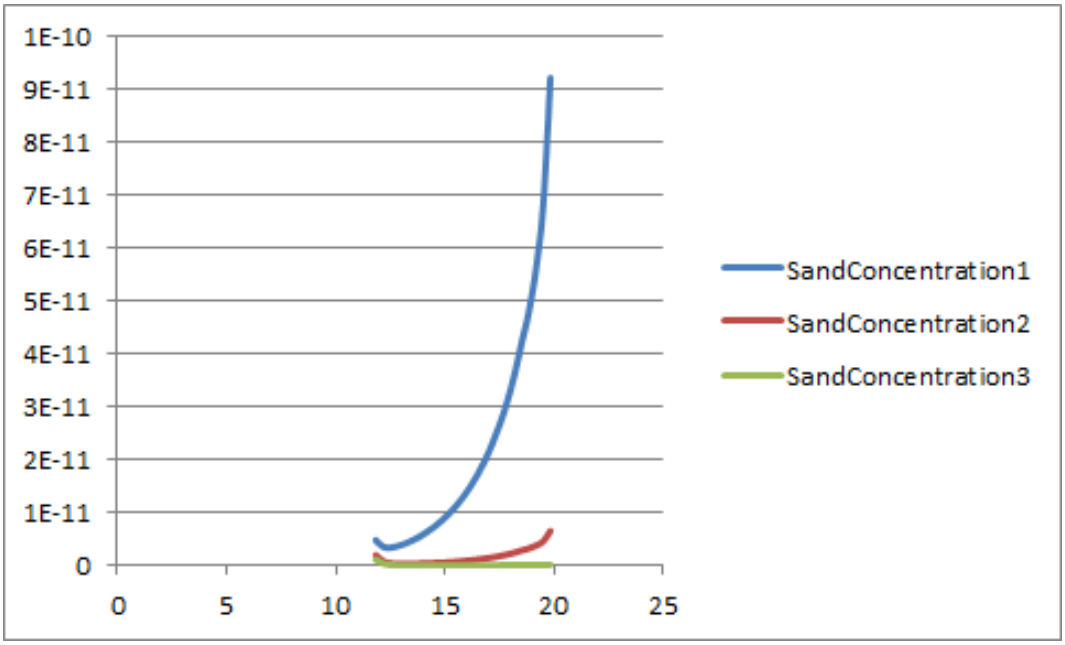

Figure 4.8 Sand concentrations at 12th load case when R=0.15, 2, 2.5mm

Above results are based on the conditions of rock elasticity (E) as 30GPa, sand radius as meshed 40/70 0.15mm, 30/50 0.2mm and 20/40 0.25mm, sand density 2.65g/cm^3, fluid viscosity as 1cp and fluid pressure 1MPa is applied in the 12 load cases. Sand and fluid velocities at 12th load cases are studied, and sand concentration at 12th is plotted when fluid and sand velocity are small enough to occupy further.

From figures 4.5 and 4.6, sand and fluid velocities at 12th load case when R=0.15, 2, 2.5mm are graphed. According to these curves, based on the only change of sand radius, the variation of sand velocity is bigger than fluid velocity. Meanwhile, smaller radius sand could obtain much higher velocity during the transport process. By contrast, these three fluid velocities curves are almost overly

on each other.

From Figure 4.7 of sand concentration at 12th load case when R=0.15, 2, 2.5mm, sand radius is not a big influence factor for sand concentration when the radius range is from 0.15mm to 2.5mm. However, figure 4.8 indicates smaller radius sand could obtain relative higher sand concentration when approaching to the last 5 meter of the fracture.

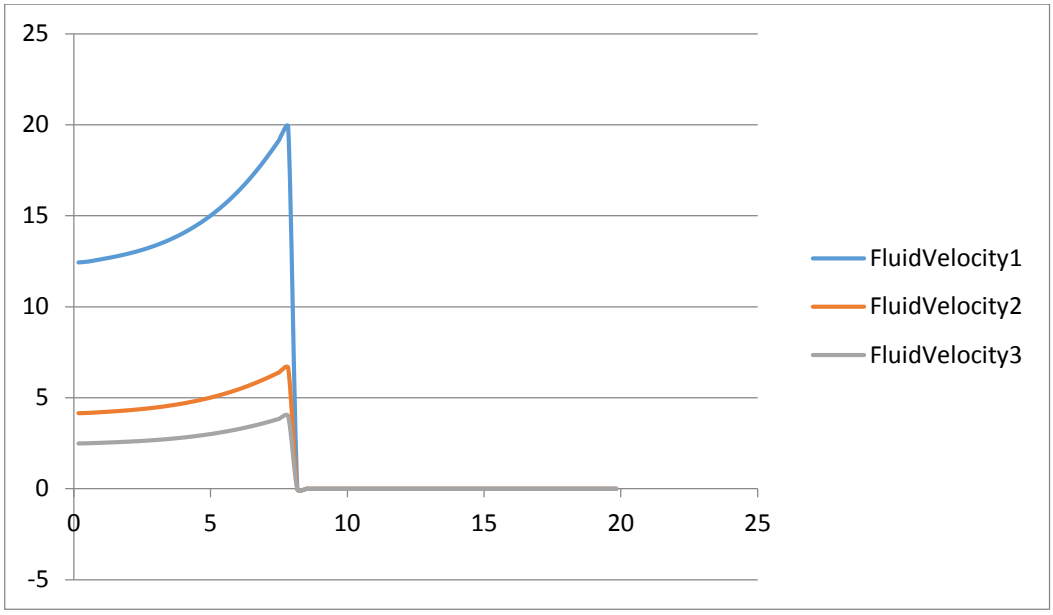

Figure 4.9 Fluid velocities at 1st load case when μ=1, 3, 5cp

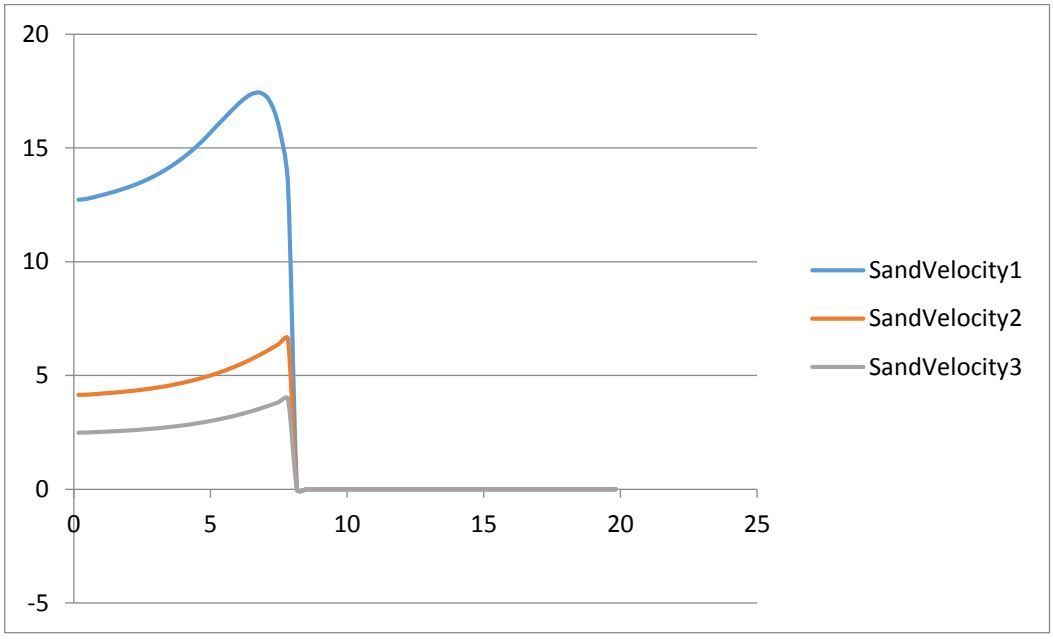

Figure 4.10 Sand velocities at 1st load case when μ=1, 3, 5cp

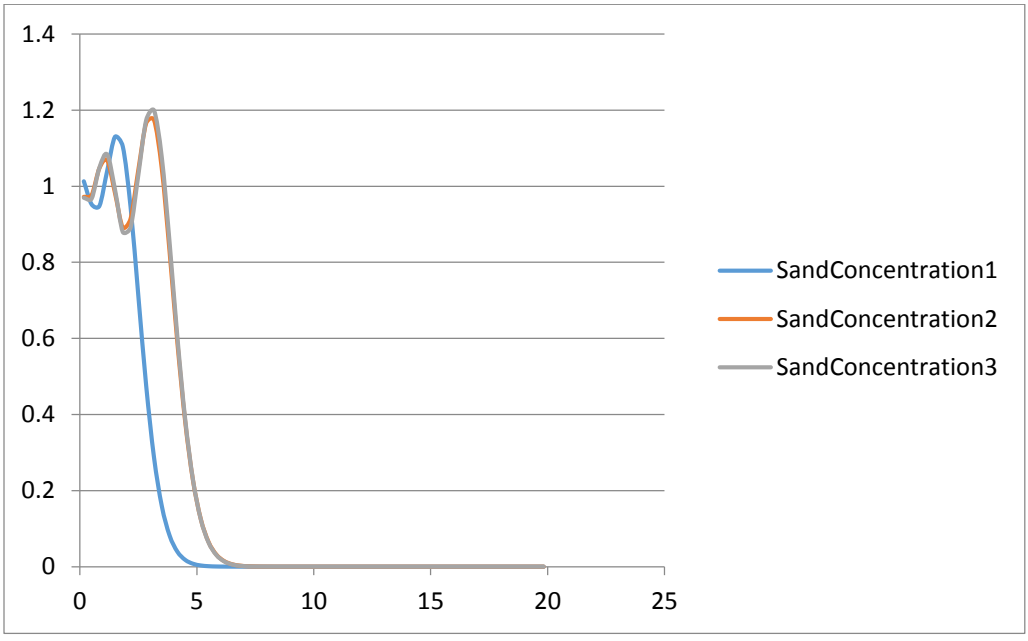

Figure 4.11 Sand concentration at 12th load case when μ=1, 3, 5cp

Above results are based on the conditions of rock elasticity (E) as 30GPa, sand radius as meshed 40/70 0.15mm, sand density 2.65g/cm^3, fluid viscosity as 1, 3, 5cp, and fluid pressure 1MPa is applied in the 12 load cases. Sand and fluid velocities at 1st load cases are studied, and sand concentration at 12th is plotted when fluid and sand velocity are small enough to occupy further.

From figure 4.9 and 4.10, fluid and sand velocities at 1st load case when μ=1, 3, 5cp indicate that the smaller the viscosity is the higher velocity could be, since high viscosity could increase the drag force and decrease the acceleration of the fluid and sand.

From figure 4.11, sand concentrations at 12th load case when μ=1, 3, 5cp mean that high fluid viscosity in the range of 1-5cp could improve the sand distribution from the whole 20m fracture. However, at the perforation area small viscosity could lead to high concentration since low viscosity at 1st load case could increase high velocity. When passing the perforation area, higher viscosity fluid could distribute more sand to the further area.

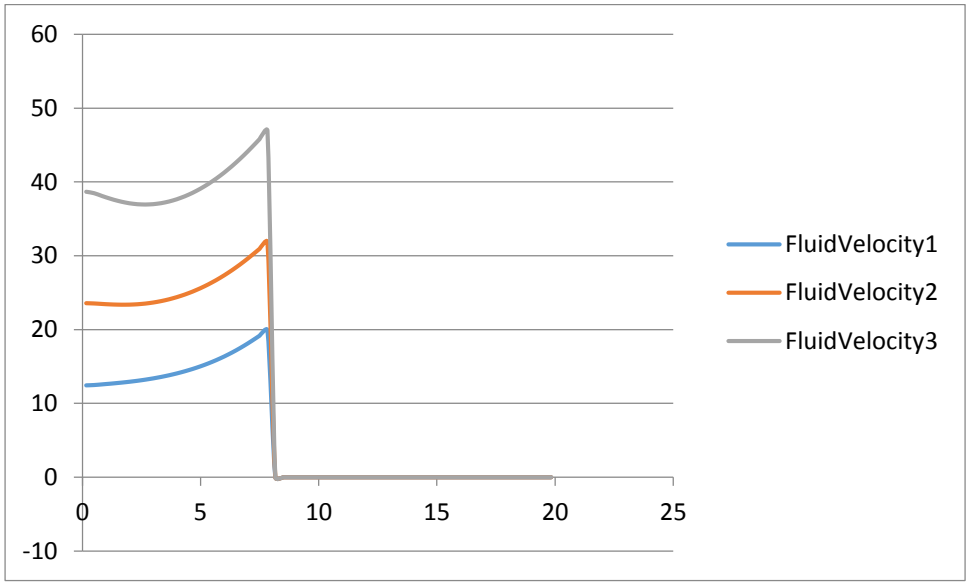

Figure 4.12 Fluid velocities at 1st load case when P=1, 2, 3MPa

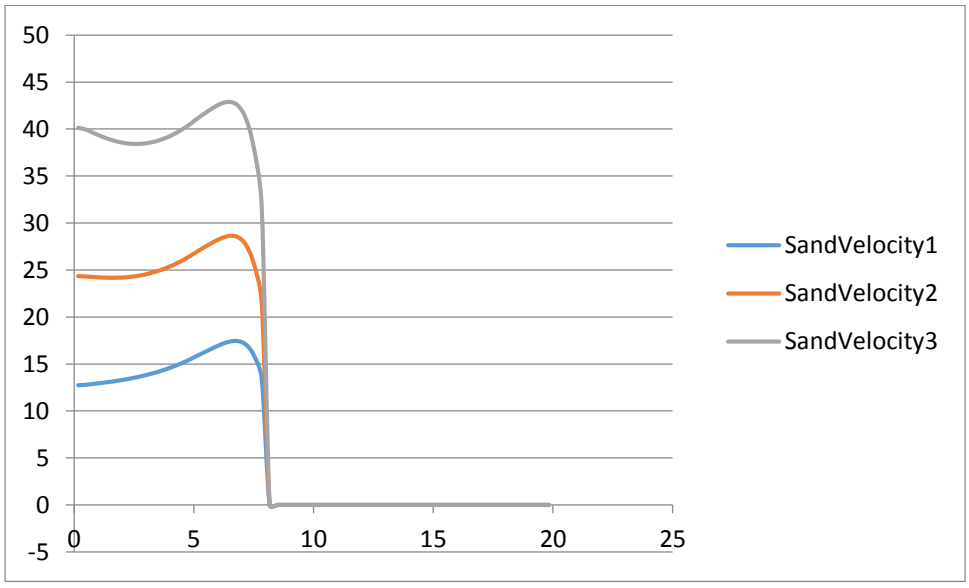

Figure 4.13 Sand velocities at 1st load case when P=1, 2, 3MPa

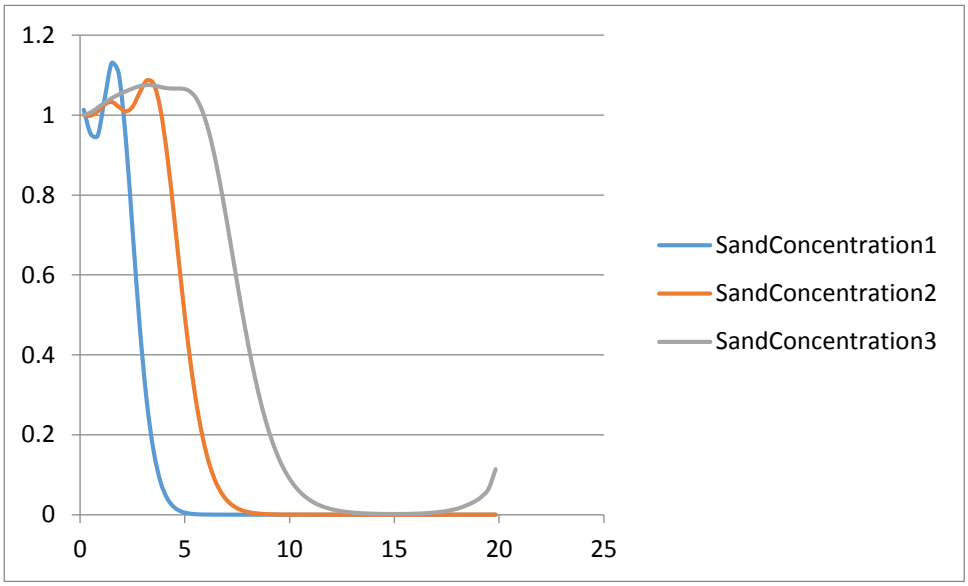

Figure 4.14 Sand concentrations at 12th load case when P=1, 2, 3MPa

Above results are based on the conditions of rock elasticity (E) as 30GPa, sand radius as meshed 40/70 0.15mm, sand density 2.65g/cm^3, fluid viscosity as 1cp, and fluid pressure 1, 2, 3 MPa are applied in the 12 load cases. Sand and fluid velocities at 1st load cases are studied, and sand concentration at 12th is plotted when fluid and sand velocity are small enough to occupy forward.

From figure 4.12 and 4.13, fluid and sand velocities at 1st load case when P=1, 2, 3MPa evidently indicate that the high pressure fluid could lead to high sand and fluid velocities.

From figure 4.14, sand concentrations at 12th load case when P=1, 2, 3MPa mean that high fluid pressure could increase sand concentration on the whole

fracture, and effectively move the high sand concentration from the perforation to the end of the fracture.

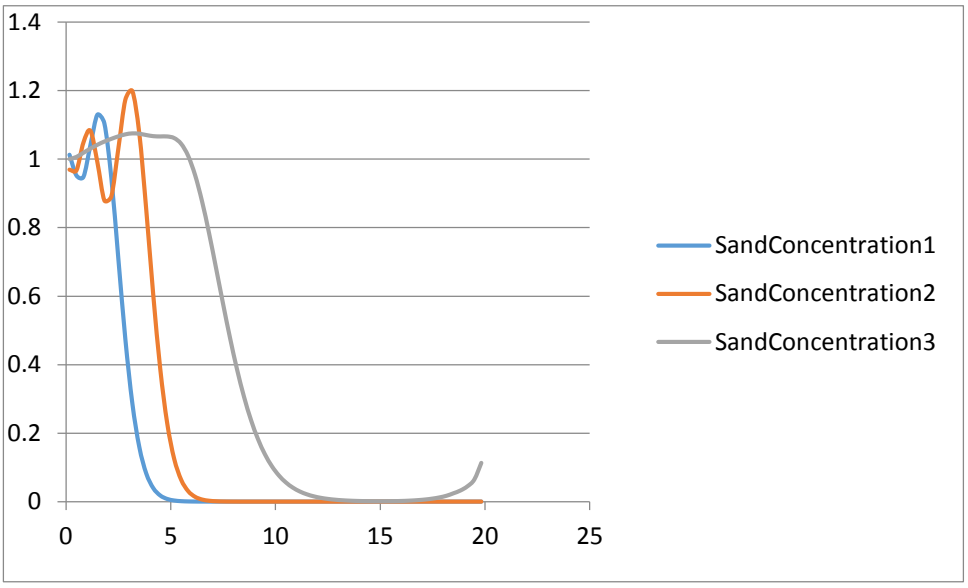

Figure 4.15 Sand concentrations at 12^{th} load case when $R = 1.5mm, \mu =$ 3cp and P=3MPa

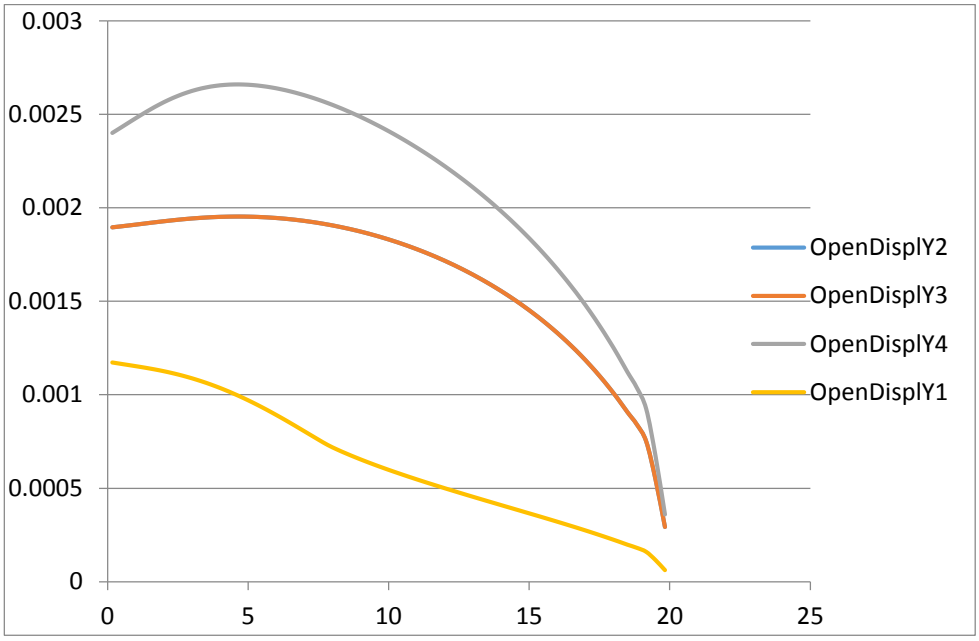

Figure 4.16 Open displacements at 1st and 12th load cases when R = 1.5mm, μ = 3cp and P=3MPa.

Above results are based on the conditions of rock elasticity (E) as 30GPa, sand density 2.65g/cm^3. Sand concentrations at 12th are plotted when fluid and sand velocity are small enough to occupy forward, fracture displacements at 1st and 12th load cases are studied.

From figure 4.15, those three curves are based on the above discussion about radius, fluid viscosity and pressure's influence on sand concentration. The results indicate that the factor of fluid pressure is more significant than viscosity and radius, and fluid viscosity is better than sand radius.

From figure 4.16, comparing open displacements 2-4 to 1 could result the conclusion that fluid pressure fluid pressure increases more big fracture space than

the function of viscosity and radius, and viscosity and radius have the same influence for fracture displacement.

Chapter 5

Conclusion

Fracture propagation, fluid flow and sand distribution are researched by analyzing their properties and interaction in this study. The Linear Elastic Fracture Mechanics (LEFM) approach is employed to understand fracture created by energized fluid. Simulation is calculated by the Boundary Element Method (BEM). Reynolds number and P*é*clet number are two important definitions for sand's inertial force over viscous force, advective transport rate over diffusive transport rate respectively. The factors, Sand radius, fluid viscosity and pressure are investigated for improving sand concentration. Based on the data and charts, those conclusions could be summarized as: smaller radius sand, high viscosity fluid (<5cp) and high pressure fluid could transport sand further; generally, fluid pressure has more significant influence on sand concentration and fracture displacement than fluid viscosity and sand radius.

References

[1] Ben E. Law and Charles W. Spencer, 1993, "Gas in tight reservoirs-an emerging major source of energy," in David G. Howell (ed.), The Future of Energy Gasses, US Geological Survey, Professional Paper 1570, p.233-252

[2] Andrews, Anthony; et al. (30 October 2009). Unconventional Gas Shales: Development, Technology, and Policy Issues. Congressional Research Service. pp. 7; 23. Retrieved 22 February 2012.

[3] T.T. Palisch, Carbo Ceramics, M.C. Vincent and P.J. Handren. "Slickwater fracturing: food for thought". SPE 115766 presented at the SPE European Formation Damage Conference, Denver, CO, 21–24 September 2008.

[4] F. Guo, N.R.Morgenstern, and J.D.Scott. "Interpretation of hydraulic fracturing breakdown pressure". Int. J. Rock Mech. Min. Sci. & Geomeeh. Abstr. Vol. 30, No. 6, pp. 617-626, 1993

[5] Shigekazu Kusumoto1 and Agust Gudmundsson (2014) Displacement and stress fields around rock fractures opened by irregular overpressure variations. *Front. Earth Sci*. 2:7. doi: 10.3389/feart.2014.00007

[6] A. Raimbay, T. Babadagli and E. Kuru. "Effect of fracture roughness and shear displacement on permeability and proppant transportation in a single fracture". SPE-171577-MS presented at the SPE/CSUR Unconventional Resources Conference - Canada held in Calgary, Alberta, Canada 2014.

[7] Nonnan R. Warpinski, Richard A. Schmidt and David A. Northrop. "In-Situ

Stresses: The Predominant Influence on Hydraulic Fracture Containment". JOURNAL OF PETROLEUM TECHNOLOGY, 0149·2136/82/0003·8932 (1982).

[8] R. Wu, O. Kresse, X. Weng, C. Cohen and H. Gu. "Modeling of interaction of hydraulic fracture in complex fracture networks". SPE 152052 presented at the SPE Hydraulic Fracturing Technology Conference held in the Woodlands, Texas, USA, 6-8 February 2012.

[9] L. Fan, J.W. Thompson and J.R. Robinson. "Understanding gas production mechanism and effectiveness of well stimulation in the Haynesville shale through reservoir simulation". CSUG/SPE 136696 was presented at the SPE/CSUR Unconventional Resources & International Petroleum Conference held in Calgary, Alberta, Canada 2010.

[10] M. S. BRUNO and F. M. NAKAGAWA. "Pore Pressure Influence on Tensile Fracture Propagation in Sedimentary Rock". Int. J. Rock Mech. Min. Sci. & Geomech. Abstr. Vol. 28, No. 4. pp. 261-273. 1991.

[11] H. Gu, X, Weng, J. Lund, M. Mack, U. Ganguly and R. Suarez-Rivera. "Hydraulic fracture crossing natural fracture at non-orthogonal angles, a criterion, its validation and applications". SPE 139984 presented at the SPE Hydraulic Fracturing Technology Conference and Exhibition held in the Woodlands, Texas, USA, 24-26 January 2011.

[12] Donald Kundert and Mike Mullen. "Proper Evaluation of Shale Gas Reservoirs

Leads to More Effective Hydraulic-Fracture Stimulation". Paper SPE 123586-MS presented at APE Rocky Mountain Petroleum Technology Conference, Denver, CO 14 – 16 April 2009.

[13] Kan Wu and Jon E. Olson. “Investigation of critical in situ and injection factors in multi-frac treatments: guidelines for controlling fracture complexity”. SPE 163821 presented at the SPE Hydraulic Fracturing Technology Conference held in the Woodlands, Texas, USA, 4-6 February 2013.

[14] B.M. Davidson, B.F. Saunders. B.M. Robinson and S.A. Holditch. "Analysis of Abnormally High Fracture Treating Pressures Caused by Complex Fracture Growth”. SPE 26154 presented at the SPE Gas Technology Symposium held in Calgary, Alberta, Canada, 28-30 June 1993.

[15] C.N. Fredd, S.B. McConnell, C.L. Boney, and K.W. England. "Experimental Study of Hydraulic Fracture Conductivity Demonstrates the Benefits of Using Proppants”. SPE 60326 presented at the 2000 SPE Rocky Mountain Regional/Low Permeability Reservoirs Symposium held in Denver, CO, 12–15 March 2000.

[16] C. Cipolla, X. Weng, M. Mack, U. Ganguly, H. Gu, O. Kresse and C. Cohen. “Integrating microseismic mapping and complex fracture modeling to characterize fracture complexity”. SPE 140185 presented at the SPE Hydraulic Fracturing Technology Conference and Exhibition held in the Woodlands, Texas, USA, 24-26 January 2011.

[17] C. Cipolla, M.J. Williams, X. Weng, X. Mack and S. Maxwell. “Hydraulic fracture monitoring to reservoir simulation maximizing value". Paper SPE 133877 presented at the SPE Technical Conference and Exhibition held in the Florence, Italy, 19-22 September 2010.

[18] D.K. Lowe, J. L. Huitt and Members Aime. “Propping agent transport in horizontal fractures”. SPE 1285 presented at the SPE Annual Fall Metting held in Denver, CO, Oct. 3-6, 1965.

[19] A. Acharya. “Particle transport in viscous and viscoelastic fracturing fluids”. SPE 13179 presented at the Annual Technical Conference and Exhibition held in Houston, Sept. 16-19 1984.

[20] Peter E. Clark and Jamal A. Quadir. “Prop transport in hydraulic fractures: a critical review of particle settling velocity equations”. SPE 9866 presented at the 1981 SPEIDOE Low Permeability Symposium held in Denver, Colorado, May 27·29, 1981.

[21] Jing Xiang. Thesis “A PKN hydraulic fracture model study and formation permeability determination”. Masters Thesis, 2011.

[22] Anton Nikolaev Kamenov. “The effect of proppant size and concentration on hydraulic fracture conductivity in shale reservoirs”. Masters Thesis, 2013.

[23] Jinlin, Zhang "Computational Fluid Dynamics (CFD) modeling of proppant transport in a plug-and-perf completion with different perforation phasing". masters Thesis. Paper 7285, 2014.

[24] Russell L. Detwiler and Harihar Rajaram. "Solute transport in variable-aperture fractures: An investigation of the relative importance of Taylor dispersion and macro dispersion". WATER RESOURCES RESEARCH, VOL. 36, NO. 7, PAGES 1611-1625, JULY 2000.

[25] Yang, B., and K. Ravi-Chandar. "Evaluation of elastic T-stress by the stress difference method." Engineering Fracture Mechanics 64.5 (1999): 589-605.

[26] Chen, Zuorong. "An ABAQUS implementation of the XFEM for hydraulic fracture problems". Effective and Sustainable Hydraulic Fracturing, 725-739, 2013.

Biographical information

The author of this thesis obtained his undergraduate degree at Southwest Jiao Tong University, China. His area was mechanical engineering with emphasis on 3D Structure Design, Stress Analysis and Manufacturing Technology. After finishing his bachelor degree, he worked at China Ming Yang Wind Power Ltd for Two years as a project administrator. He Experienced in hoisting, debugging and maintenance wind turbine, and coordinating relationship with consumers. Since January 2014, he has been pursuing on his graduate program in Mechanical Engineering at the University of Texas at Arlington. He has passion on Finite Element Methods, Fracture Mechanics, and Fluid Mechanics.